This is a preprint of: "Anomalous wave structure in magnetized materials described by non-convex equations of state", Susana Serna, Antonio Marquina, *Phys. Fluids*, vol. 26, 016101, 2014.
DOI: [10.1063/1.4851415]

Anomalous wave structure in magnetized materials described by non-convex equations of state

Susana Serna[1, a)] and Antonio Marquina[2, b)]

[1)] *Departament de Matematiques, Universitat Autonoma de Barcelona, 08193 Bellaterra-Barcelona, Spain*

[2)] *Departamento de Matematicas, Universidad de Valencia, 46100 Burjassot, Valencia, Spain*

(Dated: 28 November 2013)

We analyze the anomalous wave structure appearing in flow dynamics under the influence of magnetic field in materials described by non-ideal equations of state. We consider the system of magnetohydrodynamics equations closed by a general equation of state (EOS) and propose a complete spectral decomposition of the fluxes that allows us to derive an expression of the nonlinearity factor as the mathematical tool to determine the nature of the wave phenomena. We prove that the possible formation of non-classical wave structure is determined by both the thermodynamic properties of the material and the magnetic field as well as its possible rotation. We demonstrate that phase transitions induced by material properties do not necessarily imply the loss of genuine nonlinearity of the wavefields as is the case in classical hydrodynamics. The analytical expression of the nonlinearity factor allows us to determine the specific amount of magnetic field necessary to prevent formation of complex structure induced by phase transition in the material. We illustrate our analytical approach by considering two non-convex EOS that exhibit phase transitions and anomalous behavior in the evolution. We present numerical experiments validating the analysis performed through a set of one-dimensional Riemann problems. In the examples we show how to determine the appropriate amount of magnetic field in the initial conditions of the Riemann problem to transform a thermodynamic composite wave into a simple nonlinear wave.

Keywords: magnetohydrodynamics; non-convex equation of state; phase transitions; complex wave structure; composite waves

[a)] Author to whom correspondence should be addressed.; Electronic mail: serna@mat.uab.es

[b)] Electronic mail: marquina@uv.es

I. INTRODUCTION

Simulation codes to solve physical processes in fluid dynamics are based on nonlinear hyperbolic systems of conservation laws as Euler and magnetohydrodynamics (MHD) equations. The fluid equations describe conservation of mass, momentum, energy and magnetic field in the latter case and are closed with the constitutive relations represented by an equation of state (EOS) defining the equilibrium thermodynamic properties of the considered material. Hydrodynamic models are considered to simulate applications involving the response of solids at high pressure where the dynamic properties of the material are characterized by an EOS[1–3].

The ideal EOS framework has been traditionally used in theoretical and numerical studies because of its simplicity and convenience in simulation codes[4–10]. Nevertheless, the ideal EOS does not represent laboratory environments as well as non-ideal equations of state do. Non-ideal equations of state provide more realistic descriptions of the materials and the models representing them are more difficult to analyze and use in simulation codes[11–20].

The study of the wave dynamics in magnetohydrodynamics is essential to understand physical processes like the ones performed in laboratory experiments associated to high density physics, material processing and astrophysical phenomena. Magnetic acceleration is the basis of magnetic pinch facilities where large magnetic pressure is used to compress material samples[21–25]. Magnetic field is also commonly used to process materials in industry. Metallurgical MHD include, among other applications, magnetic stirring, magnetic damping and magnetic destabilization of liquid-liquid interfaces[2,3,26]. Magnetic outflows, accretion disks, the evolution of stellar collapse supernovae are examples of astrophysical scenarios where states of matter at extreme high densities and strong magnetic field are involved in the evolution[18,25,27]. The study of the shock wave phenomena and material response at high pressure and strong magnetic field is commonly addressed by means of fluid models of compressible flows closed with non-ideal EOSs. The understanding of these models is a challenge and a research area of interest with important applications in industry, geophysics and astrophysics among other areas[1–3,15–18,21–27].

The analysis of the wave structure in the evolution of classical hydrodynamics described by Euler equations closed with a non-ideal EOS has been widely studied in the literature[1,13,14,28–32]. It is well known that the structure and dynamics of waves are deter-

mined by the properties of the material through a thermodynamic magnitude, the fundamental derivative $\mathcal{G}$

$$\mathcal{G} := -\frac{1}{2} V \frac{\frac{\partial^2 P}{\partial V^2}\big|_S}{\frac{\partial P}{\partial V}\big|_S} \tag{1}$$

where V is the specific volume ($V \equiv \frac{1}{\rho}$, ρ the density), S the specific entropy and P the pressure. $\mathcal{G}$ measures the convexity of isentropes in the pressure-volume plane[32,33]. In this context it is common to refer as convex EOS to those characterizing materials with strictly positive fundamental derivative and non-convex EOS to those with negative one at some state in the thermodynamic plane.

The acoustic waves in classical hydrodynamics are genuinely nonlinear when the fundamental derivative is positive[12,30,33]. This implies that the only possible waves allowed in the solution are linear waves (contacts), compression shock waves and expansion fans. In hydrodynamics the convexity of the EOS determines the convex dynamics of the system. Most materials satisfy a strictly positive fundamental derivative. In other cases, where the material undergoes phase transitions or the fluid is near the critical point region, non-convex dynamics arise. Then isentropes lose convexity implying a loss of genuine nonlinearity of the acoustic waves and a negative value of the fundamental derivative. The acoustic wave family becomes more complex and the solution may generate anomalous structures like shock waves attached to an expansion fan, double shocks separated by a rarefaction fan and double rarefaction fans separated by a shock wave[29,32,34,35]. The emerging of composite wave structures (typical in non-convex dynamics) where shocks break expansion fans might not be a desirable effect in some applications. For example, in material processing, composite waves represent the loss of continuity in the medium and in consequence inhomogeneities, small cavities and porosity surfaces appear.

In the work of Lax[36,37] the concepts of genuine and non-genuine nonlinearity of the acoustic waves are generalized to hyperbolic systems of conservation laws. Decoupling the system of hyperbolic conservation laws into characteristic wavefields these are classified through an expression named nonlinearity factor that measures the monotonicity of the characteristic wave speeds along wave curves. Positive nonlinearity factor implies genuine nonlinearity of the nonlinear wavefields. In Euler dynamics it is proved that the nonlinearity factor is proportional to the fundamental derivative and therefore change of sign of this thermodynamic magnitude determines the same for the nonlinearity factor[12,14]. This relation

is not longer valid when magnetic field is involved in the physical system under study.

The MHD system of equations is a system of hyperbolic conservation laws that results from coupling Euler equations of hydrodynamics and Maxwell equations[38,39]. One of the main properties of the MHD system is that the rotation of the magnetic field may induce non-genuine nonlinearity in some characteristic wavefields. It has been analytically proved for the case of the MHD system closed with convex EOSs that the nonlinearity factor vanishes in isolated points depending on the values of the magnetic field[5,8,40]. MHD systems closed with convex EOSs may exhibit anomalous wave structure because of the rotation of the magnetic field. Let us point out that, in this case, the non-convex dynamics of the system arises because of the orientation of the magnetic field and not because of the thermodynamic properties inherited from the EOS.

In this work we focus on the characterization of the convexity of the MHD system closed with non-convex EOSs. We explore the shock wave structure and discern the influence of thermodynamic properties of materials and magnetic field on the formation of complex wave structures.

In our analysis we consider the MHD system of equations governed by a general EOS. We provide an analytical expression of the nonlinearity factor for the nonlinear wavefields and prove that the loss of genuine nonlinearity of the wavefields depends on both: the thermodynamic properties of the material and the magnetic field. We demonstrate that phase transitions might not imply the loss of genuine nonlinearity. We also show that complex wave structure induced by the loss of thermodynamic convexity can be neutralized by prescribing a specific amount of magnetic field. Indeed, we prove that the non-convex thermodynamic behavior induced by a non-convex EOS in a hydrodynamics system can be reverted into convex dynamics by introducing an appropriate intensity of magnetic field in the system.

We illustrate our analytical approach considering the MHD system and two non-convex EOS that exhibit anomalous behavior. We analyze a van der Waals model that exhibits phase transition[28,30] and a Mie-Grüneisen type EOS[1,41,42] which is considered as representative of real liquids and solids for which the fundamental derivative changes sign. In both cases we analyze the structure and behavior of wave curves determined by the nonlinearity factor. We present numerical experiments validating the analytical approach through a set of one-dimensional Riemann problems. Firstly we show examples exhibiting non-convex

dynamics in the absence of magnetic field and secondly we display their MHD counterparts where the magnetic field has been chosen to revert the non-convex dynamics into convex and therefore eliminating complex wave structure.

The characterization of the wave structure of the MHD system closed with a general EOS presented in this paper provides a better understanding of the influential role of the magnetic field in the dynamics of these complex flows. Our study might help to improve characteristic-based code capabilities to simulate processes relevant in high energy-density laboratory astrophysics where high power lasers (not well approximated by the ideal gas EOS) are used to study jets and bow shocks. The proposed approach can also be of interest in industrial applications of material processing when the properties of the material are described through a non-convex EOS. Our characterization provides a mathematical tool that might guide to predict the intensity of magnetic drive to increase pressure in a system and therefore avoid shocks and other unwanted wave structures (loss of homogeneity in a sample) intrinsic to non-convex dynamics.

The paper is organized as follows. In Sec. II we review general concepts on nonlinear hyperbolic systems of conservation laws. Sec. III is devoted to the analysis of the wave structure of MHD systems closed by a general equation of state where we derive a simple expression of the nonlinearity factor in terms of the fundamental derivative and the magnetic field. Sec. IV includes numerical examples of anomalous wave structure in magnetized materials described by a van der Waals EOS and a Mie-Grüneisen EOS. In Sec. V we draw our conclusions.

II. NONLINEAR HYPERBOLIC SYSTEMS OF CONSERVATION LAWS

In this Section we review general concepts on the theory of nonlinear hyperbolic systems of conservation laws necessary to develop our study on the MHD wave structure under a general EOS.

Mathematical models in fluid dynamics are represented by hyperbolic systems of conservation laws of the form

$$\frac{\partial \mathbf{u}}{\partial t} + \nabla \cdot \mathbf{F}(\mathbf{u}) = 0 \tag{2}$$

where $\mathbf{u}$ is the vector of m conserved variables and $\mathbf{F}(\mathbf{u})$ is the corresponding one of m fluxes. The system is hyperbolic if the Jacobians of the fluxes in any direction are diagonalizable

matrices with real eigenvalues and a complete set of eigenvectors in each neighborhood of the solution[36,37,39,43].

In one dimension the eigenvalues of the Jacobian of the flux $\mathbf{f}(\mathbf{u})$, $\mathbf{f}'(\mathbf{u})$, are denoted as $\lambda_1(\mathbf{u}), \cdots, \lambda_m(\mathbf{u})$ counting each one as many times as its multiplicity. The complete system of right and left eigenvectors are defined as $R_{\mathbf{u}} = \{\mathbf{r}_1(\mathbf{u}), \cdots, \mathbf{r}_m(\mathbf{u})\}$ and $L_{\mathbf{u}} = \{\mathbf{l}_1(\mathbf{u}), \cdots, \mathbf{l}_m(\mathbf{u})\}$ respectively diagonalizing $\mathbf{f}'(\mathbf{u})$ such that $\mathbf{r}_i \cdot \mathbf{l}_j = \delta_{ij}$ and

$$L_{\mathbf{u}}(\mathbf{u})\, \mathbf{f}'(\mathbf{u})\, R_{\mathbf{u}}(\mathbf{u}) = \Lambda = \mathrm{diag}(\lambda_1(\mathbf{u}), \cdots, \lambda_m(\mathbf{u})) \tag{3}$$

The diagonalization of the Jacobians evaluated at same state decouples the linearized hyperbolic system in m scalar conservation laws defining the so-called local characteristic fields and their corresponding local characteristic fluxes[36,37]. The system is closed by an EOS defining the thermodynamic properties of the material.

The eigenvalues of the Jacobian represent the characteristic speeds of the characteristic fluxes analogous to the first derivative of the flux of a scalar conservation law. The nonlinearity of the corresponding characteristic fields is determined by the scalar quantity called *nonlinearity factor*

$$\sigma_k(\mathbf{u}) \equiv \nabla_{\mathbf{u}} \lambda_k(\mathbf{u}) \cdot \mathbf{r}_k(\mathbf{u}) \tag{4}$$

where $\lambda_k(\mathbf{u})$ and $\mathbf{r}_k(\mathbf{u})$ are the kth characteristic field eigenvalue and eigenvector of the Jacobian $\mathbf{f}'(\mathbf{u})$ respectively. This magnitude corresponds to the second derivative of the scalar flux in a scalar conservation law[36,37,43].

The characteristic wavefields are classified as *linearly degenerate*, $\sigma_k(\mathbf{u}) = 0\,, \forall \mathbf{u}$, *genuinely nonlinear (convex)* $\sigma_k(\mathbf{u}) \neq 0\,, \forall \mathbf{u}$ and *non-genuinely nonlinear (non-convex)* when $\sigma_k(\mathbf{u})$ vanishes in isolated points $\mathbf{u_0}$.

Convex hyperbolicity occurs when characteristic fields are either linear or genuinely nonlinear. In convex dynamics the wave structure consists only of contacts, shocks and rarefaction waves.

Non-convex hyperbolicity occurs when genuinely nonlinear fields become non-genuinely nonlinear. The loss of genuine nonlinearity results in anomalous wave structure such composite (combination of smooth and discontinuous solutions), shock and rarefaction waves[1,11–14].

It is well known in classical hydrodynamics represented by Euler equations that the nonlinearity factor of nonlinear wavefields can be written in the equivalent form

$$\sigma_{\pm}(\mathbf{u}) = \pm \frac{a}{\rho}\, \mathcal{G} \tag{5}$$

where $\mathcal{G}$ is the fundamental derivative, Eq. (1),

$$a = \sqrt{\left.\frac{\partial P}{\partial \rho}\right|_S} \tag{6}$$

is the acoustic sound speed, P the pressure, ρ the density and S the specific entropy.

In Euler hydrodynamics the qualitative character of the solution of the conservation laws depends on the thermodynamic properties of the material. From Eq. (5) it is clear that in the case of hydrodynamics a change of sign of the fundamental derivative implies a change of sign of the nonlinearity factor and therefore non-convex hyperbolicity and the consequent anomalous wave structure.

In the following Section we analyze the wave structure of the MHD system of hyperbolic conservation laws closed by a general EOS.

III. ANOMALOUS WAVE STRUCTURE IN NON-IDEAL MHD EQUATIONS

The thermodynamic properties of a material have a decisive effect on the nature of the shock wave phenomena that appears in it. In classical hydrodynamics the nature of the EOS determines the behavior of the wave structure. In a region of negative value of the fundamental derivative the dynamics might exhibit non-classical wave phenomena. The case of MHD shock wave dynamics is more involved. Apart from the influence of the specific material in the possible formation of anomalous wave structure, the presence of the magnetic field adds complexity to the nonlinear wave dynamics. It has been proved in ideal MHD that hyperbolic singularities appear when the magnetic field rotates causing the MHD eigensystem to induce non-genuine nonlinearity in some of the nonlinear wavefields[5,6,8,40,44]. In this Section we perform a complete analytical study of the MHD wave structure under a general EOS. We present a full spectral decomposition of the Jacobians of the fluxes and derive an expression of the nonlinearity factor for the nonlinear wavefields. We then analyze the dependency of the non-genuinely nonlinear behavior of the shock wave phenomena in terms of the fundamental derivative and the magnetic field.

The MHD system of equations for real gases can be expressed as

$$\frac{\partial \rho}{\partial t} + \nabla \cdot (\rho \mathbf{v}) = 0 \tag{7a}$$

$$\frac{\partial}{\partial t}(\rho \mathbf{v}) + \nabla \cdot \left(\rho \mathbf{v}\mathbf{v}^T + (P + \frac{1}{2}\mathbf{B}^2) I - \mathbf{B}\mathbf{B}^T \right) = 0 \tag{7b}$$

$$\frac{\partial \mathbf{B}}{\partial t} - \nabla \times (\mathbf{v} \times \mathbf{B}) = 0 \tag{7c}$$

$$\frac{\partial E}{\partial t} + \nabla \cdot \left(\left(E + P - \frac{1}{2}\mathbf{B}^2 \right) \mathbf{v} - (\mathbf{v} \times \mathbf{B}) \times \mathbf{B} \right) = 0 \tag{7d}$$

where $\rho, \mathbf{v} = (u, v, w), \mathbf{B} = (B_x, B_y, B_z)$ and E denote the mass density, the velocity field, the magnetic field and the total energy respectively, being $\mathbf{u} = (\rho, \rho u, \rho v, \rho w, B_x, B_y, B_z, E)$ the vector of conserved variables. The energy is expressed as

$$E = \rho\varepsilon + \frac{1}{2}\rho q^2 + \frac{1}{2}\mathbf{B}^2 \tag{8}$$

where q^2 and $\mathbf{B}^2$ are the squares of the magnitudes of the velocity field and the magnetic field respectively and ε the specific internal energy. $P = P(\rho, \varepsilon)$ is the hydrodynamic pressure defined through a real gas EOS. The system is completed with a condition on the magnetic field, the divergence free constraint

$$\nabla \cdot \mathbf{B} = 0. \tag{9}$$

Let us define $(b_x, b_y, b_z) = (B_x, B_y, B_z)/\sqrt{\rho}$ and $b^2 = b_x^2 + b_y^2 + b_z^2$. The general expression of the square of the acoustic sound speed (6) is given by

$$a^2 = P_\rho + P_\varepsilon \frac{P}{\rho^2}$$

where P_ρ represents the partial derivative of P with respect to ρ and P_ε the partial derivative of P with respect to ε. The specific total enthalpy is defined as

$$h^* = \frac{E + P^*}{\rho} \tag{10}$$

where $P^* = P + \frac{1}{2}\mathbf{B}^2$ is the total pressure.

We propose a complete spectral decomposition of the MHD system (7) for the one-dimensional case under a general equation of state. In the one-dimensional case the divergence free constraint (9) is reduced to the case where B_x is constant. The constancy of B_x implies that this quantity is considered an initial condition acting as a parameter. Thus the evolution equation for the x-component of the magnetic field is not solved. The system of equations provides an eigensystem composed of seven waves: one entropy wave, two Alfvén

waves and four magnetoacoustic waves. Their corresponding eigenvalues λ, left eigenvectors $\mathbf{l}$ and right eigenvectors $\mathbf{r}$ are defined as follows.

The spectral decomposition reflects the dependency of the wave structure on the magnetic field $\mathbf{B}$ and on the thermodynamics induced by the EOS through magnitudes a^2 and the Grüneisen coefficient[33],

$$\Gamma = \frac{P_\varepsilon}{\rho} \tag{11}$$

The Alfven wave speed is denoted by $c_A = |b_x|$ and the fast and slow wave speeds are given by

$$c_{f,s} = \sqrt{\frac{1}{2}\left((a^2+b^2) \pm \sqrt{(a^2+b^2)^2 - 4a^2b_x^2}\right)} \tag{12}$$

The eight characteristic wave speeds associated to the system (7) are: $\lambda_1(\mathbf{u}) = u - c_f$, $\lambda_2(\mathbf{u}) = u - c_A$, $\lambda_3(\mathbf{u}) = u - c_s$, $\lambda_4(\mathbf{u}) = u$, $\lambda_5(\mathbf{u}) = u + c_s$, $\lambda_6(\mathbf{u}) = u + c_A$, $\lambda_7(\mathbf{u}) = u + c_f$.

Depending on the direction and magnitude of the magnetic field, these wave speeds may coincide making the MHD equations a non-strictly hyperbolic system of conservation laws. Thus, the set of eigenvectors of the system can be singular at the points where the eigenvalues are degenerate. From the original approach by Jeffrey and Taniuti[38] the eigensystem of the MHD equations closed with an ideal EOS has been extensively studied with the purpose of proposing different normalizations avoiding these singularities[5–8,40].

In this section we propose a set of eigenvectors which are an extension to the general EOS case of the ones presented for ideal MHD in[8]. The latter approach exhibits an scaled version of the complete system of eigenvectors proposed by Brio and Wu[5,40] and therefore are well defined providing a proper normalization to avoid singularities at the points where the eigenvalues are degenerate. Our scaling also guarantees continuity of the eigenvectors with respect to the conserved variables in the neighborhood of singular points[8].

We present a unified expression for the eigenvectors of the nonlinear characteristic wavefields. We define $\mathrm{sgn}(t) = 1$ for $t \geq 0$ and $\mathrm{sgn}(t) = -1$ otherwise and set β_y and β_z values from

$$\beta_y = \begin{cases} \frac{B_y}{\sqrt{B_y^2+B_z^2}}; & B_y^2 + B_z^2 \neq 0 \\ \frac{1}{\sqrt{2}}; & \text{otherwise} \end{cases} \qquad \beta_z = \begin{cases} \frac{B_z}{\sqrt{B_y^2+B_z^2}}; & B_y^2 + B_z^2 \neq 0 \\ \frac{1}{\sqrt{2}}; & \text{otherwise} \end{cases}$$

The right and left eigenvectors associated to the fast ($k = 1, 7$) and slow ($k = 3, 5$) magnetoacoustic wavefields with eigenvalues $\lambda_1, \lambda_3, \lambda_5$ and λ_7, can be written for $k = 1, 3, 5, 7$ respectively as

$$\mathbf{r}_k = \Bigg(\alpha,\ \alpha(u+c),\ \alpha v - \bar{\alpha}\bar{c}\,\mathrm{sgn}(c^2-a^2)\,\mathrm{sgn}(B_x)\beta_y,\ \alpha w - \bar{\alpha}\bar{c}\mathrm{sgn}(c^2-a^2)\mathrm{sgn}(B_x)\beta_z,$$
$$\bar{\alpha}\frac{a}{\sqrt{\rho}}\ \mathrm{sgn}(c^2-a^2)\beta_y,\ \bar{\alpha}\frac{a}{\sqrt{\rho}}\,\mathrm{sgn}(c^2-a^2)\beta_z,$$
$$\alpha\Big(h^* - a^2 - b^2 + c^2 + uc\Big) - \mathrm{sgn}(c^2-a^2)\bar{\alpha}\bar{c}\,\mathrm{sgn}(B_x)(v\beta_y + w\beta_z)\Bigg)^T \tag{13}$$

$$\mathbf{l}_k = \frac{1}{2a^2}\Bigg(\Gamma\alpha\Big(\frac{a^2}{\Gamma} + q^2 + b^2 - h^*\Big) - \alpha uc + \mathrm{sgn}(c^2-a^2)\bar{\alpha}\bar{c}\,\mathrm{sgn}(B_x)(v\beta_y + w\beta_z), -\Gamma\alpha u + \alpha c,$$
$$-\Gamma\alpha v - \bar{\alpha}\bar{c}\,\mathrm{sgn}(c^2-a^2)\,\mathrm{sgn}(B_x)\beta_y, -\Gamma\alpha w - \bar{\alpha}\bar{c}\,\mathrm{sgn}(c^2-a^2)\,\mathrm{sgn}(B_x)\beta_z,$$
$$-\Gamma\alpha B_y + \sqrt{\rho}\,a\bar{\alpha}\ \mathrm{sgn}(c^2-a^2)\beta_y, -\Gamma\alpha B_z + \sqrt{\rho}\,a\bar{\alpha}\,\mathrm{sgn}(c^2-a^2)\beta_z, \Gamma\alpha\Bigg) \tag{14}$$

where c and $\bar{c}$ and α and $\bar{\alpha}$ are determined as:

- for $k = 1$ and $k = 7$, $c = \mp c_f$, $\bar{c} = \mp c_s$ and

$$\alpha = \begin{cases} \alpha_f \cdot \mathrm{sgn}(B_y); & a < c_A \\ \alpha_f; & \text{otherwise} \end{cases} \qquad \bar{\alpha} = \begin{cases} \alpha_s \cdot \mathrm{sgn}(B_y); & a < c_A \\ \alpha_s; & \text{otherwise} \end{cases}$$

- for $k = 3$ and $k = 5$, $c = \mp c_s$, $\bar{c} = \mp c_f$ and

$$\alpha = \begin{cases} \alpha_s \cdot \mathrm{sgn}(B_y); & a > c_A \\ \alpha_s; & \text{otherwise} \end{cases} \qquad \bar{\alpha} = \begin{cases} \alpha_f \cdot \mathrm{sgn}(B_y); & a > c_A \\ \alpha_f; & \text{otherwise} \end{cases}$$

and α_f and α_s are defined from the following expressions

$$\alpha_f = \begin{cases} \frac{\sqrt{a^2-c_s^2}}{\sqrt{c_f^2-c_s^2}};\ B_y^2 + B_z^2 \neq 0 \,\text{or}\, c_A \neq a \\ \frac{1}{\sqrt{2}}; \qquad \text{otherwise} \end{cases} \qquad \alpha_s = \begin{cases} \frac{\sqrt{c_f^2-a^2}}{\sqrt{c_f^2-c_s^2}}\ B_y^2 + B_z^2 \neq 0 \,\text{or}\, c_A \neq a \\ \frac{1}{\sqrt{2}}; \qquad \text{otherwise} \end{cases}$$

We define $\tau = \frac{\Gamma}{a^2}$ to express the eigenvector associated to linear wavefield λ_4 as

$$\mathbf{r}_4 = \left(1, u, v, w, 0, 0, h^* - b^2 - \frac{a^2}{\Gamma}\right)^T$$
$$\mathbf{l}_4 = \tau\left(\frac{1}{\tau} + \frac{1}{2}\Big(h^* - b^2 - \frac{a^2}{\Gamma} - q^2\Big), u, v, w, B_y, B_z, -1\right)$$

The eigenvectors associated to the Alfven wavefields with eigenvalues λ_2 and λ_6 are expressed as proposed in Ref.[38] as

$$\mathbf{r}_2 = \left(0, 0, -\beta_z \text{sgn}(B_x), \beta_y \text{sgn}(B_x), -\frac{\beta_z}{\sqrt{\rho}}, \frac{\beta_y}{\sqrt{\rho}}, -\text{sgn}(B_x)(\beta_z v - \beta_y w)\right)^T$$

$$\mathbf{r}_6 = \left(0, 0, -\beta_z \text{sgn}(B_x), \beta_y \text{sgn}(B_x), \frac{\beta_z}{\sqrt{\rho}}, -\frac{\beta_y}{\sqrt{\rho}}, -\text{sgn}(B_x)(\beta_z v - \beta_y w)\right)^T$$

$$\mathbf{l}_2 = \left(\frac{1}{2}\text{sgn}(B_x)(\beta_z v - \beta_y w), 0, -\frac{\beta_z}{2}\text{sgn}(B_x), \frac{\beta_y}{2}\text{sgn}(B_x), -\beta_z\frac{\sqrt{\rho}}{2}, \beta_y\frac{\sqrt{\rho}}{2}, 0\right)$$

$$\mathbf{l}_6 = \left(\frac{1}{2}\text{sgn}(B_x)(\beta_z v - \beta_y w), 0, -\frac{\beta_z}{2}\text{sgn}(B_x), \frac{\beta_y}{2}\text{sgn}(B_x), \beta_z\frac{\sqrt{\rho}}{2}, -\beta_y\frac{\sqrt{\rho}}{2}, 0\right)$$

The proposed complete system of eigenvectors is continuous with respect to the conserved variables similarly as defended in Ref.[8] for ideal MHD.

The extension of this seven wave eigensystem to the multidimensional case of the MHD system under a general equation of state such that it satisfies the eight wave approach by Powell et. al[7] is obtained in a simple manner. Similarly as explained in[6], the extended left eigenvectors $l_{1,8}$, $l_{2,7}$, $l_{3,6}$ and l_4 are obtained, respectively, by inserting into $l_{1,7}$, $l_{2,6}$, $l_{3,5}$ and l_4 of the seven wave eigensystem and a $5th$ component whose value is $-\Gamma\alpha B_x$. Likewise the right eigenvectors $r_{1,8}$, $r_{2,7}$,$r_{3,6}$ and r_4 are obtained, respectively, by adding a $5th$ component with a null value to $r_{1,7}$, $r_{2,6}$,$r_{3,5}$ and r_4 of the seven wave eigensystem. In addition, l_5 and r_5 are given by

$$\mathbf{r}_5 = (0, 0, 0, 0, 1, 0, 0, B_x)^T, \qquad \mathbf{l}_5 = (0, 0, 0, 0, 1, 0, 0, 0, 0)$$

The system of eigenvectors for the Jacobian of the flux in the $y-$ direction can be obtained by interchanging B_x by B_y, u by v, the second component by the third and the fifth by the sixth.

From the expression of the nonlinear right eigenvectors (13) we can derive the nonlinearity factor for the nonlinear wavefields and study the wave structure of the MHD system under a general EOS.

Let us first provide a thermodynamic relation that will be useful in the derivation of the nonlinearity factor of the nonlinear wavefields. The following identity links the component of the gradient of the specific internal energy in the direction of any nonlinear right eigenvector with a thermodynamic relation that appears in the calculation of derivatives at constant specific entropy with respect to density of thermodynamic magnitudes.

Lemma 1 *Let $\mathbf{r}_c(\mathbf{u})$ represent the right nonlinear eigenvector of the Jacobian of the MHD system and ε the specific internal energy. The following thermodynamic relation is satisfied*

$$\nabla_{\mathbf{u}}\,\varepsilon\cdot\mathbf{r}_c(\mathbf{u})=\alpha\frac{P}{\rho^2} \tag{15}$$

Proof. We consider equation (8) to obtain an expression for the specific internal energy $\varepsilon=\frac{E}{\rho}-\frac{1}{2}q^2-\frac{1}{2\rho}\mathbf{B}^2$. We calculate the gradient of the specific internal energy with respect to the conserved variables:

$$\nabla_{\mathbf{u}}\,\varepsilon=\Big(\frac{\partial\varepsilon}{\partial u_j}\Big)_{j=1}^{7}=\frac{1}{\rho}\Big(\frac{1}{2}q^2-\varepsilon,-u,-v,-w,-B_y,-B_z,1\Big) \tag{16}$$

Using expression (13) and considering $D=\bar{\alpha}\bar{c}\,\mathrm{sgn}\,(c^2-a^2)\mathrm{sgn}(B_x)$ and $E=\bar{\alpha}\frac{a}{\sqrt{\rho}}\mathrm{sgn}(c^2-a^2)$ to simplify notation, the scalar product becomes

$$\begin{aligned}\nabla_{\mathbf{u}}\,\varepsilon\cdot\mathbf{r}_c(\mathbf{u})=\frac{1}{\rho}\Bigg(&\alpha\Big(\frac{1}{2}q^2-\varepsilon\Big)-\alpha u^2-\alpha uc-\alpha v^2+D\beta_y v-\alpha w^2+D\beta_z w-Eb_y\beta_y\\&-Eb_z\beta_z+\alpha(h^*-a^2-b^2+uc+c^2)-D(\beta_y v+\beta_z w)\Bigg)\\=\frac{\alpha}{\rho}\Big(&\frac{1}{2}q^2-\varepsilon-q^2-uc+h^*-a^2-b^2+uc+c^2\Big)-\frac{E}{\rho}(B_y\beta_y+B_z\beta_z)\end{aligned}$$

Then, from expressions (10) and (8), substituting E and using identities $\bar{\alpha}a\,\mathrm{sgn}(c^2-a^2)=\frac{\alpha(c^2-a^2)}{\sqrt{b_y^2+b_z^2}}$, $\frac{B_y}{\sqrt{\rho}}=b_y$ and $\beta_y=\frac{b_y}{\sqrt{b_y^2+b_z^2}}$ the scalar product simplifies to

$$\begin{aligned}\nabla_{\mathbf{u}}\,\varepsilon\cdot\mathbf{r}_c(\mathbf{u})=&\frac{\alpha}{\rho}\Big(-\frac{1}{2}q^2-\varepsilon+\varepsilon+\frac{1}{2}q^2+\frac{1}{2}b^2+\frac{P}{\rho}+\frac{1}{2}b^2-a^2-b^2+c^2\Big)\\&-\frac{\bar{\alpha}a}{\sqrt{\rho}}\mathrm{sgn}(c^2-a^2)\frac{B_y\beta_y+B_z\beta_z}{\rho}\\=&\frac{\alpha}{\rho}\Big(c^2-a^2+\frac{P}{\rho}\Big)-\frac{1}{\sqrt{\rho}}\frac{\alpha(c^2-a^2)}{\sqrt{b_y^2+b_z^2}}\frac{1}{\sqrt{\rho}}\frac{b_y^2+b_z^2}{\sqrt{b_y^2+b_z^2}}\\=&\frac{\alpha}{\rho}\Big(c^2-a^2+\frac{P}{\rho}-(c^2-a^2)\Big)=\alpha\frac{P}{\rho^2}\end{aligned}$$

□

Theorem 1 (Formula of the nonlinearity factor for general MHD) *The nonlinearity factor for the nonlinear wavefields of the MHD system is expressed as*

$$\sigma_c(\mathbf{u})\equiv\nabla_{\mathbf{u}}\lambda_c(\mathbf{u})\cdot\mathbf{r}_c(\mathbf{u})=\frac{\alpha c}{\rho}(\alpha^2\mathcal{G}+\frac{3}{2}\bar{\alpha}^2) \tag{17}$$

where $\lambda_c(\mathbf{u})=u+c$ with $c=\pm c_{f,s}$ is the eigenvalue corresponding to a fast (f) or slow (s) characteristic field, $\mathbf{r}_c(\mathbf{u})$ the associated right eigenvector, $\mathcal{G}$ is the fundamental derivative and α and $\bar{\alpha}$ are defined following the normalization of the nonlinear wavefields.

In the case of no rotation of the magnetic field, expression (17) is simplified to

$$\sigma^{\pm}_{c_f}(\mathbf{u}) = \pm\frac{\alpha_f c_f}{\rho}\Big(\alpha_f^2\mathcal{G} + \frac{3}{2}\alpha_s^2\Big) \tag{18}$$

$$\sigma^{\pm}_{c_s}(\mathbf{u}) = \pm\frac{\alpha_s c_s}{\rho}\Big(\alpha_s^2\mathcal{G} + \frac{3}{2}\alpha_f^2\Big) \tag{19}$$

where $\lambda^{\pm}_{c_f}(\mathbf{u}) = u \pm c_f$, $\lambda^{\pm}_{c_s}(\mathbf{u}) = u \pm c_s$ *are the eigenvalues corresponding to a fast or slow characteristic wavefield,* $\mathbf{r}^{\pm}_{c_f}(\mathbf{u})$ *and* $\mathbf{r}^{\pm}_{c_s}(\mathbf{u})$ *are the associated right eigenvectors and* α_f *and* α_s *are defined following the normalization of the nonlinear wavefields.*

Proof. For the purpose of computing the scalar product $\nabla\lambda_c(\mathbf{u}) \cdot \mathbf{r}_c(\mathbf{u})$ we first calculate the expression of the vector $\nabla\lambda_c(\mathbf{u})$ where $\lambda_c = u + c$ is an eigenvalue associated to a nonlinear characteristic wavefield and c represents the fast or slow wave speeds, $\pm c_f$ or $\pm c_s$, respectively. The gradient of the eigenvalue is calculated as

$$\nabla_{\mathbf{u}}\lambda_c(\mathbf{u}) = \Big(\frac{\partial}{\partial u_j}(u + c)\Big)_{j=1}^{7} \tag{20}$$

In order to simplify the calculation of the partial derivatives of c with respect to the conserved variables u_j, $j = 1, \cdots, 7$ we use an equivalent expression of $\frac{\partial c}{\partial u_j}$. We consider the identity $\frac{\partial c^2}{\partial u_j} = 2c\frac{\partial c}{\partial u_j}$ and manipulate expression (12) as follows.

From (12) it is stated that c satisfies

$$c^4 - (a^2 + b^2)c^2 + a^2 b_x^2 = 0 \tag{21}$$

Taking partial derivatives of (21) with respect to the conserved variables u_j, $j = 1, \cdots, 7$ we have

$$\begin{aligned}&\frac{\partial}{\partial u_j}c^4 - \frac{\partial}{\partial u_j}\Big((a^2 + b^2)c^2\Big) + \frac{\partial}{\partial u_j}\Big(a^2 b_x^2\Big) = \\ &2c^2\frac{\partial c^2}{\partial u_j} - (a^2 + b^2)\frac{\partial c^2}{\partial u_j} - c^2\Big(\frac{\partial a^2}{\partial u_j} + \frac{\partial b^2}{\partial u_j}\Big) + a^2\frac{\partial b_x^2}{\partial u_j} + b_x^2\frac{\partial a^2}{\partial u_j} = 0\end{aligned} \tag{22}$$

Since c is associated to a nonlinear wavefield, we have that $2c^2 - (a^2 + b^2) = c^2 - \bar{c}^2 \neq 0$. We can then isolate $\frac{\partial c^2}{\partial u_j}$ from (22) and we obtain for $j = 1, \cdots, 7$,

$$\frac{\partial c^2}{\partial u_j} = \frac{c^2 - b_x^2}{c^2 - \bar{c}^2}\frac{\partial a^2}{\partial u_j} + \frac{c^2}{c^2 - \bar{c}^2}\frac{\partial b^2}{\partial u_j} - \frac{a^2}{c^2 - \bar{c}^2}\frac{\partial b_x^2}{\partial u_j} \tag{23}$$

Taking into account that $\frac{c^2-b_x^2}{c^2-\bar{c}^2} = \frac{c^2}{a^2}\alpha^2$ we compute the gradient of the eigenvalue $\lambda_c(\mathbf{u})$ plugging (23) into (20) and applying the chain rule as

$$\begin{aligned}\nabla_{\mathbf{u}}\lambda_c(\mathbf{u}) &= \left(\frac{\partial u}{\partial u_j} + \frac{1}{2c}\frac{\partial c^2}{\partial u_j}\right)_{i=1}^{7} = \frac{1}{2c}\left(2c\frac{\partial u}{\partial u_j} + \alpha^2\frac{c^2}{a^2}\frac{\partial a^2}{\partial u_j} + \frac{c^2}{c^2-\bar{c}^2}\frac{\partial b^2}{\partial u_j} - \frac{a^2}{c^2-\bar{c}^2}\frac{\partial b_x^2}{\partial u_j}\right)_{i=1}^{7} \\ &= \frac{1}{2c}\Bigg(-2c\frac{u}{\rho} + \alpha^2\frac{c^2}{a^2}\Big(\frac{\partial a^2}{\partial \rho} + \frac{\partial a^2}{\partial \varepsilon}\frac{\partial \varepsilon}{\partial u_1}\Big) - \frac{c^2}{c^2-\bar{c}^2}\frac{b^2}{\rho} + \frac{a^2}{c^2-\bar{c}^2}\frac{b_x^2}{\rho}, \\ &\quad 2c\frac{1}{\rho} + \alpha^2\frac{c^2}{a^2}\frac{\partial a^2}{\partial \varepsilon}\frac{\partial \varepsilon}{\partial u_2},\ \alpha^2\frac{c^2}{a^2}\frac{\partial a^2}{\partial \varepsilon}\frac{\partial \varepsilon}{\partial u_3},\ \alpha^2\frac{c^2}{a^2}\frac{\partial a^2}{\partial \varepsilon}\frac{\partial \varepsilon}{\partial u_4},\ \alpha^2\frac{c^2}{a^2}\frac{\partial a^2}{\partial \varepsilon}\frac{\partial \varepsilon}{\partial u_5} + \frac{2c^2}{c^2-\bar{c}^2}\frac{b_y}{\sqrt{\rho}}, \\ &\quad \alpha^2\frac{c^2}{a^2}\frac{\partial a^2}{\partial \varepsilon}\frac{\partial \varepsilon}{\partial u_6} + \frac{2c^2}{c^2-\bar{c}^2}\frac{b_z}{\sqrt{\rho}},\ \alpha^2\frac{c^2}{a^2}\frac{\partial a^2}{\partial \varepsilon}\frac{\partial \varepsilon}{\partial u_7}\Bigg) \end{aligned} \tag{24}$$

The nonlinearity factor is obtained through the scalar product between (24) and (13) by using identities $\bar{\alpha}a\,\mathrm{sgn}(c^2-a^2) = \frac{\alpha(c^2-a^2)}{\sqrt{b_y^2+b_z^2}}$ and $b_x\frac{c}{a} = \bar{c}\,\mathrm{sgn}(B_x)$,

$$\begin{aligned}\sigma_c(\mathbf{u}) = -\frac{\alpha}{\rho}u + \frac{\alpha(u+c)}{\rho} + \frac{1}{2c}\Bigg(&\alpha^2\frac{c^2}{a^2}\left(\frac{\partial a^2}{\partial \rho}\alpha + \frac{\partial a^2}{\partial \varepsilon}\sum_{j=1}^{7}\mathbf{r}_c(u)_j\frac{\partial \varepsilon}{\partial \mathbf{u}_j}\right) \\ &-b^2\frac{c^2}{c^2-\bar{c}^2}\frac{\alpha}{\rho} + \frac{a^2}{c^2-\bar{c}^2}b_x^2\frac{\alpha}{\rho} + \frac{2c^2}{c^2-\bar{c}^2}\frac{\alpha}{\rho}(c^2-a^2)\Bigg)\end{aligned} \tag{25}$$

Then, we first substitute the value of $\nabla_{\mathbf{u}}\varepsilon\cdot\mathbf{r}_c(\mathbf{u})$ accordingly with Lemma 1 and second we identify $\frac{\partial a^2}{\partial \rho} + \frac{P}{\rho^2}\frac{\partial a^2}{\partial \varepsilon}$ with $\frac{\partial a^2}{\partial \rho}\Big|_S$ and $\bar{\alpha} = \frac{c^2-a^2}{c^2-\bar{c}^2}$

$$\begin{aligned}\sigma_c(\mathbf{u}) &= \alpha\frac{c}{\rho} + \frac{1}{2c}\left(\alpha^3\frac{c^2}{a^2}\left(\frac{\partial a^2}{\partial \rho} + \frac{P}{\rho^2}\frac{\partial a^2}{\partial \varepsilon}\right) + \frac{c^2}{c^2-\bar{c}^2}\frac{\alpha}{\rho}\Big(2c^2 - 2a^2 - b^2 + \frac{a^2b_x^2}{c^2}\Big)\right) \\ &= \alpha\frac{c}{\rho} + \frac{1}{2c}\left(\alpha^3\frac{c^2}{a^2}\frac{\partial a^2}{\partial \rho}\Big|_S + \frac{\alpha}{\rho}\bar{\alpha}^2c^2\right)\end{aligned} \tag{26}$$

From the equivalent expression of the fundamental derivative $\mathcal{G} = 1 + \frac{\rho}{a}\frac{\partial a}{\partial \rho}\Big|_S$ and the facts that $\frac{\partial a^2}{\partial \rho}\Big|_S = 2a\frac{\partial a}{\partial \rho}\Big|_S$ and $\alpha^2 + \bar{\alpha}^2 = 1$ we can rewrite (26) as

$$\begin{aligned}\sigma_c(\mathbf{u}) &= \frac{\alpha c}{\rho} + \frac{\alpha c}{2\rho}\Big(\frac{\alpha^2}{a^2}\rho\frac{\partial a^2}{\partial \rho}\Big|_S + \bar{\alpha}^2\Big) = \frac{\alpha c}{\rho}\Big(1 + \frac{1}{2}\frac{\alpha^2}{a^2}2\rho a\frac{\partial a}{\partial \rho}\Big|_S + \frac{\bar{\alpha}^2}{2}\Big) \\ &= \frac{\alpha c}{\rho}\Big(\alpha^2\mathcal{G} + \frac{3}{2}\bar{\alpha}^2\Big)\end{aligned}$$

□

Remark 1 *An alternative dimensionless expression of the nonlinearity factor (17) could be derived if the general expression of the right eigenvectors (13) was multiplied by $\frac{\rho}{c}$ (the left eigenvectors should be consequently multiplied by $\frac{c}{\rho}$). However, with this normalization the*

eigensystem would not be complete since the eigenvectors would present singularities when $c = c_s$ degenerates to zero at singular points.

Remark 2 *Let us remark that the expressions of the nonlinearity factors, Eqs. (18) and (19), differ from the corresponding one for the hydrodynamic case, Eq. (5), on terms that depend on the magnetic field.*

The following corollaries describe particular cases of special relevance.

Corollary 1 *Let* $\mathbf{B}$ *be a magnetic field with* $B_x \neq 0$ *and* $B_y^2 + B_z^2 \neq 0$ *and no rotation and let the fundamental derivative* $\mathcal{G} < 0$*. The following cases apply*

1. *If* $-\frac{3}{2} < \mathcal{G} < 0$ *at some point then there exists a* $\delta > 0$ *such that if* $\rho a^2 - \delta \leq \mathbf{B}^2 \leq \rho a^2 + \delta$ *then the nonlinearity factors are both positive and therefore the wave structure is classical.*

2. *If* $\mathcal{G} < -\frac{3}{2}$ *at some point then at least one of the nonlinear wavefields induces a negative nonlinearity factor and therefore there might be anomalous wave structure.*

Proof:

In order to demonstrate both statements we first shall prove that both nonlinearity factors are non-negative if and only if

$$\mathcal{G} \geq -\frac{3}{2} \min\left(\frac{\alpha_s^2}{\alpha_f^2}, \frac{\alpha_f^2}{\alpha_s^2}\right) \tag{27}$$

Indeed, by hypothesis $0 < \alpha_s^2 < 1$ and $0 < \alpha_f^2 < 1$. The non-negativity of nonlinearity factors is satisfied if

$$\alpha_f^2 \mathcal{G} + \frac{3}{2}\alpha_s^2 \geq 0 \qquad \text{and} \qquad \alpha_s^2 \mathcal{G} + \frac{3}{2}\alpha_f^2 \geq 0$$

Both inequalities are fulfilled if and only if $\mathcal{G} \geq -\frac{3}{2} \min\left(\frac{\alpha_s^2}{\alpha_f^2}, \frac{\alpha_f^2}{\alpha_s^2}\right)$

In order to prove the first assertion we use the explicit expressions

$$\frac{\alpha_s^2}{\alpha_f^2} = \frac{c_f^2 - a^2}{a^2 - c_s^2}$$

obtained from the definitions of α_s^2 and α_f^2. Then, using the formulas of the fast and slow wave speeds we have that

$$\frac{\alpha_s^2}{\alpha_f^2} = \frac{\sqrt{(a^2 - b^2) + 4a^2(b^2 - b_x^2)} - (a^2 - b^2)}{\sqrt{(a^2 - b^2) + 4a^2(b^2 - b_x^2)} + (a^2 - b^2)}$$

From this expression it is straightforward to see that $a^2 = b^2 \iff \alpha_s^2 = \alpha_f^2 = \frac{1}{2}$ and $a^2 > b^2$ ($a^2 < b^2$ respectively) if and only if $\alpha_s^2 < \alpha_f^2$ ($\alpha_s^2 > \alpha_f^2$). Since $\mathbf{B}^2 = \rho b^2$, we have that

$$\lim_{\mathbf{B^2}\to\rho a^2} \frac{\alpha_s^2}{\alpha_f^2} = 1 = \lim_{\mathbf{B^2}\to\rho a^2} \frac{\alpha_f^2}{\alpha_s^2} \tag{28}$$

We set $\epsilon = 1 - \frac{2}{3}|\mathcal{G}| > 0$. From the definition of limit in (28) we can find a $\delta > 0$ such that if $\rho a^2 - \delta \leq \mathbf{B}^2 \leq \rho a^2 + \delta$ then $\left|1 - \frac{\alpha_s^2}{\alpha_f^2}\right| < \epsilon$ and $\left|1 - \frac{\alpha_f^2}{\alpha_s^2}\right| < \epsilon$. We distinguish two cases: in the first case, $\rho a^2 - \delta \leq \mathbf{B}^2 \leq \rho a^2$, we have that $\frac{\alpha_s^2}{\alpha_f^2} \leq 1$ and $1 - \frac{\alpha_s^2}{\alpha_f^2} \leq \epsilon = 1 - \frac{2}{3}|\mathcal{G}|$ and therefore $\frac{2}{3}|\mathcal{G}| \leq \frac{\alpha_s^2}{\alpha_f^2}$. This implies that

$$\mathcal{G} > -\frac{3}{2}\frac{\alpha_s^2}{\alpha_f^2} = -\frac{3}{2}\min\left(\frac{\alpha_s^2}{\alpha_f^2}, \frac{\alpha_f^2}{\alpha_s^2}\right)$$

Thus, from (27) it follows that both nonlinearity factors are positive.

The other case, $\rho a^2 - \delta \leq \mathbf{B}^2 \leq \rho a^2$, follows using the same argument over the ratio $\frac{\alpha_f^2}{\alpha_s^2}$.

Second assertion of the Corollary follows from the fact that

$$\min\left(\frac{\alpha_s^2}{\alpha_f^2}, \frac{\alpha_f^2}{\alpha_s^2}\right) \leq 1$$

and therefore if $\mathcal{G} < -\frac{3}{2}$ at some point then (27) never holds and therefore at least one of the nonlinearity factors is negative. □

The following corollary describes the cases where nonlinear wavefields degenerate to linear wavefields depending on the magnitude and direction of the magnetic field.

Corollary 2 *The following are possible degenerate cases*

1. *If* $\mathbf{B} \equiv 0$ *(i.e.*$(B_x, B_y, B_z) = (0, 0, 0)$*), then* $\alpha_f^2 = 1$ *and* $\alpha_s^2 = 0$ *and system (7) reduces to Euler equations and therefore*

$$\sigma_{c_f}^{\pm}(\mathbf{u}) = \pm\frac{a}{\rho}\mathcal{G} \tag{29}$$

2. *Let* $B_x \neq 0$ *and* $B_y = B_z = 0$.

   (a) *If* $a > c_A$ *then* $c_f^2 = a^2$, $c_s^2 = b_x^2$, $\alpha_f^2 = 1$, $\alpha_s^2 = 0$ *and therefore*

$$\sigma_{c_f}^{\pm}(\mathbf{u}) = \pm\frac{a}{\rho}\mathcal{G}$$

   The only nonlinear wavefields are fast and the change of sign of $\mathcal{G}$ *implies non-convex hyperbolicity of the fast wavefield.*

(b) *If* $a < c_A$ *then* $c_f^2 = b_x^2$, $c_s^2 = a^2$, $\alpha_f^2 = 0$, $\alpha_s^2 = 1$ *and therefore*

$$\sigma_{c_s}^{\pm}(\mathbf{u}) = \pm\frac{a}{\rho}\mathcal{G}$$

The only nonlinear wavefields are the slow ones. Fast nonlinear wavefields degenerate to linear Alfven waves. Change of sign of $\mathcal{G}$ *implies non-convex hyperbolicity of the slow wavefield.*

(c) *If* $a = c_A$ *then* $c_f^2 = c_s^2 = a^2 + b_x^2$, $\alpha_f^2 = \frac{1}{2}$, $\alpha_s^2 = \frac{1}{2}$ *and therefore*

$$\sigma_{c_f}(\mathbf{u}) = 0 \qquad \text{and} \qquad \sigma_{c_s}(\mathbf{u}) = 0$$

Nonlinear wavefields degenerate to linear.

3. *If* $B_x = 0$ *and* $B_y^2 + B_z^2 \neq 0$ *then* $c_f^2 = a^2 + b^2$, $c_s^2 = 0$, $\alpha_f^2 = \frac{a^2}{a^2+b^2}$, $\alpha_s^2 = \frac{b^2}{a^2+b^2}$ *and therefore*

$$\sigma_{c_f}^{\pm}(\mathbf{u}) = \pm\frac{a}{\rho(a^2+b^2)}(a^2\mathcal{G} + \frac{3}{2}b^2)$$

The slow wavefield degenerates to a linear one and the only nonlinear wavefields are fast.

We summarize previous results in Table I.

Remark 3 *In case 3, if* $b^2 > \frac{2}{3}a^2|\mathcal{G}|$ *then the sign of* $a^2\mathcal{G} + \frac{3}{2}b^2$ *is positive and therefore the wave structure is genuinely nonlinear and anomalous wave structure is not given.*

Remark 4 *Corollary 2 indicates specific scenarios where the wave structure of a fluid is not influenced by the presence of the magnetic field. It also reveals the situation where a specific amount of magnetic field* $\mathbf{B}$ *can counterbalance the possible negative value of the fundamental derivative. Therefore, an appropriate prescription of magnetic field could prevent the formation of composite waves induced by phase transition in the material.*

The performed analysis provides a suitable insight on the MHD wave structure. The analysis can also be considered as a mathematical tool to determine the possibilities of transforming non-classical behavior of the wave structure in hydrodynamic simulations into classical regimes under the influence of the magnetic field. In the following Section we illustrate the above analysis considering the MHD system of equations together with two

TABLE I. Degenerate cases of the nonlinear wavefields described in Corollary 2

		c_f^2	c_s^2	α_f^2	α_s^2	Nonlinearity factor
$B_x = 0$ and $B_y^2 + B_z^2 = 0$		a^2	0	1	0	$\frac{a}{\rho}\mathcal{G}$
$B_x \neq 0$ and $B_y^2 + B_z^2 = 0$	$a > c_A$	a^2	b_x^2	1	0	$\frac{a}{\rho}\mathcal{G}$
	$a < c_A$	b_x^2	a^2	0	1	$\frac{a}{\rho}\mathcal{G}$
	$a = c_A$	b_x^2	b_x^2	$\frac{1}{2}$	$\frac{1}{2}$	0
$B_x = 0$ and $B_y^2 + B_z^2 \neq 0$		$a^2 + b^2$	0	$\frac{a^2}{a^2+b^2}$	$\frac{b^2}{a^2+b^2}$	$\frac{a}{\rho(a^2+b^2)}(a^2\mathcal{G} + \frac{3}{2}b^2)$

non-convex EOS. For each of them we analyze the wave structure for Riemann problems as the tool to investigate phenomena associated with shocks and expansion waves and their interactions.

IV. NUMERICAL EXAMPLES OF ANOMALOUS WAVE STRUCTURE IN MAGNETIZED MATERIALS

In this Section we consider two analytical models of non-convex EOS namely the van der Waals and the Mie-Grüneisen to illustrate the analysis performed in the previous Section. Van der Waals and Mie-Grüneisen models are simple models to investigate phenomena related to negative nonlinearity[1,15–17,29,34,35]. We particularize the study for each non-convex model performing numerical experiments showing the anomalous wave phenomena that appears in the evolution of specific Riemann problems proposed in the literature for hydrodynamic codes. We extend these Riemann problems to planar magnetohydrodynamics scenarios ($B_z = 0$) prescribing specific amounts of magnetic field in the initial conditions that allow to modify the wave structure preventing the formation of thermodynamical composite

waves.

In order to determine the amount of magnetic field needed to change the wave structure in each scenario we take into account case 1 of Corollary 1 and case 3 of Corollary 2. Case 1 in Corollary 1 asserts that positive nonlinearities are obtained for the fast and slow wavefields when the fundamental derivative keeps negative values in $]-\frac{3}{2},0[$ and the oblique magnetic field ($B_x \neq 0$ and $B_y^2 + B_z^2 \neq 0$) does not rotate and is confined to a bounded corona region. On the other hand following case 3 in Corollary 2 we can obtain positive nonlinearity for a specific amount of transversal magnetic field ($B_x = 0$ and $B_y^2 + B_z^2 \neq 0$) and any negative value of the fundamental derivative.

We are going to consider different hydrodynamic problems in which anomalous structure effects due to negative nonlinearities appear in the simulation. In order to revert a non-classical hydrodynamics wave structure into a classical regime we use either of these results. The general way we proceed is as follows.

We run the hydrodynamics code for the problem under study at a certain time t_* and examine the profile of the fundamental derivative. As the present wave dynamics is anomalous, the thermodynamical variable holds negative values at some points of the flow field inducing negative nonlinearity in the system. We set $\mathcal{G}_{\min}(<0)$ the minimum value of the fundamental derivative in our hydrodynamical scene and look up the values of the density ρ and the square of the acoustic sound speed a^2 at the same position and time and label them ρ_* and a_*^2 respectively. We use two practical criteria to estimate the amount of magnetic field that counterbalances the negative weight of the fundamental derivative in (18) and (19) so that we obtain positive values of the nonlinearity terms. Consequently the non-classical behavior in the hydrodynamics scenario is reverted into a classical one in the MHD framework. The practical criteria read as follows.

Practical criterion 1: Following case 1 in Corollary 1, if $\mathcal{G}_{\min} \in]-\frac{3}{2},0[$ we apply an oblique magnetic field to the hydrodynamics initial data such that its magnitude is $\mathbf{B}^2 \approx a_*^2\rho_*$ with $B_x > 0$ and $B_y > 0$. Then the appearing wave structure in the MHD scene is entirely classical. In this case where the $x-$component of the magnetic field is present the slow nonlinear wavefield is activated and a more involved wave structure appears.

Note that for large or very small amounts of oblique magnetic field such that $\mathbf{B}^2$ is not confined into the corona region defined in Corollary 1 the negative weight of the fundamental derivative cannot be counterbalanced and therefore nonlinearity terms remain negative and

anomalous wave structure might appear.

Practical criterion 2: Following case 3 in Corollary 2, for $\mathcal{G}_{min} < 0$ we apply a transversal magnetic field ($B_x = 0$) with $B_y > \sqrt{\frac{2}{3}|\mathcal{G}_{\min}|a_*^2\rho_*}$. Then the non-classical phenomena is turned into a classical regime. Note that in this case there is not lower bound condition for the minimum value of the fundamental derivative.

The evolution of the MHD system with either the oblique or the transversal magnetic field as prescribed in the practical criteria together with the initial data of density, velocity, and pressure as in the purely hydrodynamical original problem will provide a classical wave structure at the considered time t_*.

Next we present several numerical examples of hydrodynamics problems and their extended magnetohydrodynamics versions where the magnetic field has been determined following the practical criteria described above.

In order to perform numerical simulations we extend to general MHD the shock capturing scheme presented in Ref.[8] for ideal MHD. The high order numerical scheme is based on the Marquina Flux Formula (MFF) as Riemann solver[9]. The flux formulation has been proved to behave robust in multiple scenarios[8,10,18–20,25,45,46]. It computes the numerical fluxes at cell interfaces by means of two linearizations at each side of the interface following the Marquina's interface strategy. The procedure satisfies Rankine-Hugoniot relations approximately and avoids the computation of arithmetic averages to define intermediate states as it is common in other Riemann solvers when Roe linearizations are not available[4]. We implement to high order accuracy in space following the Shu-Osher flux formulation[47] by using a third order reconstruction procedure based on hyperbolas[48,49]. High order accuracy in time is achieved by using a third order TVD Runge-Kutta time stepping procedure[47]. Details on the implementation of the high order shock-capturing scheme for general MHD are expanded in the Appendix A.

In our hydrodynamics experiments we compute the approximate solution of the problem using the hydrodynamics version of the MHD code by setting $\mathbf{B} \equiv 0$.

A. The van der Waals model for dense fluids under the influence of magnetic field

The van der Waals gas is a model often considered in hydrodynamic scenarios to investigate phenomena related to anomalous shock wave dynamics. It represents a powerful analytical model that allows thermodynamic phase change and therefore complex wave dynamics[1,12,28,30,33,39].

The expression to define the pressure by the van der Waals EOS model is as follows. Let us define $\kappa = \frac{R}{C_V}$ where R is the gas constant, C_V is the specific heat at constant volume and $\eta_a > 0$ and $\eta_b > 0$ are positive constants accounting for the intermolecular forces and the molecule size respectively. The pressure is obtained from

$$P = \kappa \frac{\rho}{1 - \eta_b \rho}(\varepsilon + \eta_a \rho) - \eta_a \rho^2 \tag{30}$$

From this expression we can derive the thermodynamic magnitudes relevant for the wave structure analysis: the Grüneisen coefficient,

$$\Gamma = \frac{\kappa}{1 - \eta_b \rho} \tag{31}$$

the square of the acoustic sound speed

$$a^2 = \frac{\kappa(\kappa + 1)}{(1 - \eta_b \rho)^2}(\varepsilon + \eta_a \rho) - 2\eta_a \rho$$

and the fundamental derivative

$$\mathcal{G}(\rho, \varepsilon) = \frac{(\kappa + 2)(\kappa + 1)\kappa(\varepsilon + \eta_a \rho) - 6\eta_a \rho(1 - \rho\eta_b)^3}{2(\kappa + 1)\kappa(\varepsilon + \eta_a \rho)(1 - \rho\eta_b) - 4\eta_a \rho(1 - \rho\eta_b)^3} \tag{32}$$

In order to explore the wave dynamics arising in MHD systems under a van der Waals EOS we first examine the behavior of shock waves in the case of hydrodynamics described by Euler equations.

We consider three Riemann problems proposed for Euler equations in references[28,30]. The initial data for the dense gas are defined in the interval $[0, 1]$ as two constant states at both sides of 0.5, $\mathbf{u}_L$ (left) and $\mathbf{u}_R$ (right). Initial values for the density, velocity and pressure for the three dense gas problems are shown in Table II. The values of the EOS parameters are the same for the three problems: $R = 1; C_V = 80; \eta_a = 3; \eta_b = 1/3$, ($\eta_a$ and η_b are chosen such that critical pressure and critical specific volume are equal to 1).

TABLE II. Initial conditions for the Van der Waals hydrodynamics shock tube problems

	ρ_L	u_L	P_L	ρ_R	u_R	P_R
DG1	1.8181	0	3.000	0.275	0	0.575
DG2	0.879	0	1.090	0.562	0	0.885
DG3	0.879	0	1.090	0.275	0	0.575

TABLE III. Initial data for Hydrodynamics and MHD DG1 Riemann problems

HD-DG1	MHD-DG1-Oblique	MHD-DG1-Transversal
DG1 and $\mathbf{B} \equiv 0$	DG1 and $\mathbf{B} = (0.34, 0.34, 0)$	DG1 and $\mathbf{B} = (0, 0.45, 0)$

The three problems develop non-classical wave structure. In each case there exist a region where the fundamental derivative $\mathcal{G}$ is negative inducing negative nonlinearity. We are going to use these problems to show different ways of inverting the non-classical behavior of the hydrodynamic simulations into a classical wave structure by means of applying a specific amount of magnetic field in the initial conditions of the problem. In order to prescribe an appropriate intensity of magnetic field we follow the practical criteria presented previously.

Figures exhibiting results of the van der Waals dense gas Riemann problems are structured such that the first row displays the hydrodynamic simulation and second and third rows show extensions of the corresponding hydrodynamics Riemann problems to magnetohydrodynamics scenarios where the initial values of the magnetic field have been chosen following the first and second criteria respectively. All pictures in the Figures display a reference solution of the shock tube problem under study computed with 5000 grid points versus the obtained approximate solution using 800 grid points.

1. DG1 hydrodynamic and MHD Riemann problems

The initial data of the DG1 hydrodynamics Riemann problem in Table II provide positive initial states of the fundamental derivative. The thermodynamical variable becomes negative at some points of the flow evolution inducing formation of non-classical waves. Figure 1 exhibits results for the hydrodynamics and magnetohydrodynamics simulations at time

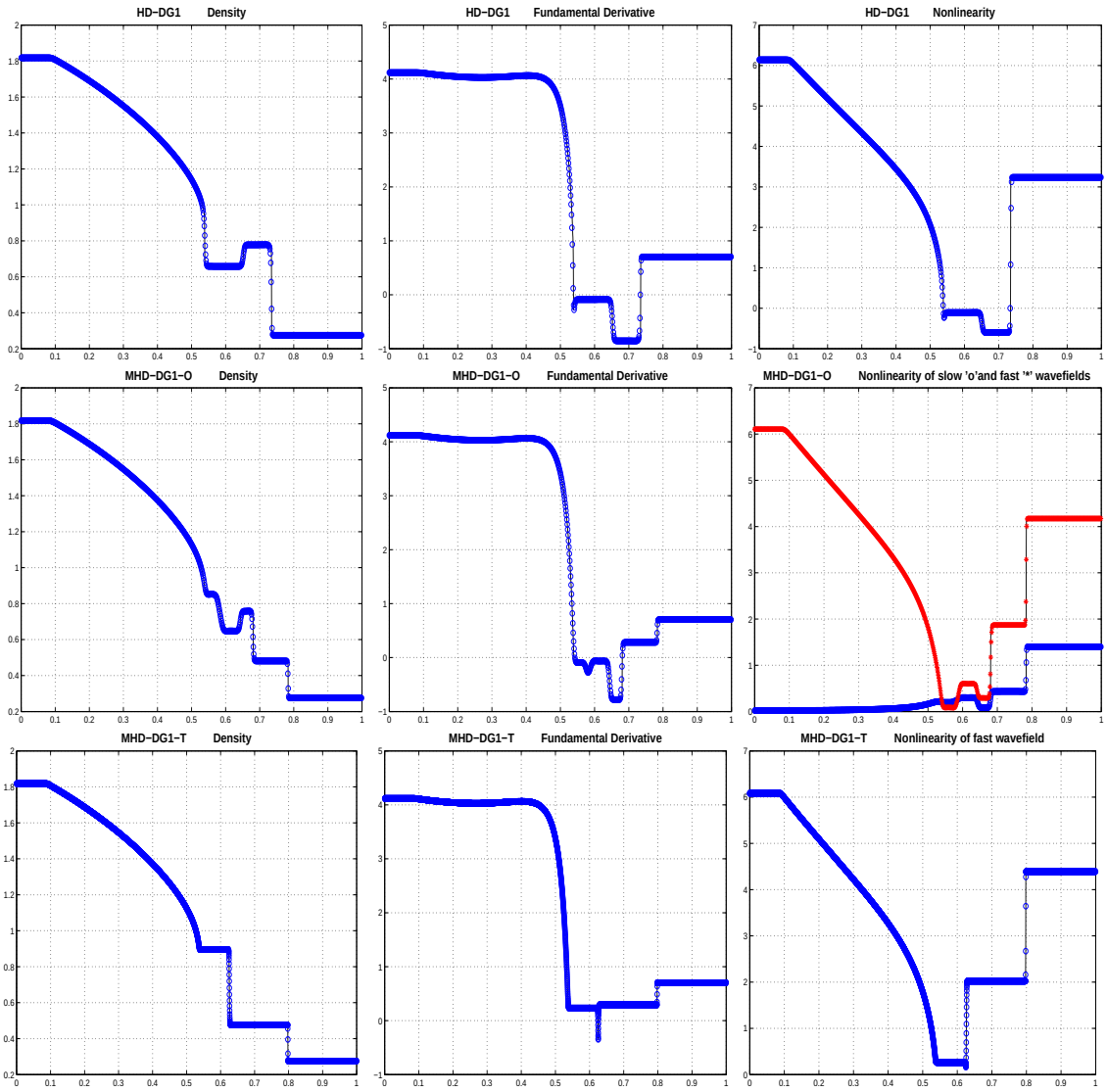

FIG. 1. Numerical solutions at time $t = 0.15$ of the Hydrodynamics and MHD van der Waals DG1 Riemann problems. First row, Hydrodynamics-DG1. Second row, MHD-DG1 with Oblique magnetic field. Third row, MHD-DG1 with Transversal magnetic field. Form left to right profiles of: density, fundamental derivative and the corresponding nonlinearity factors of nonlinear wavefields for each case.

$t_* = 0.15$. First row of Figure 1 displays the profiles of the density, fundamental derivative and nonlinearity term of the hydrodynamic simulation. The solution of the hydrodynamic problem presents a three wave structure: a contact (entropy) wave separating a compression shock wave traveling to the right and a composite wave traveling to the left. The composite wave, consisting of an expansion shock attached to an expansion fan, is located in $]0.5, 0.6[$

TABLE IV. Initial data for Hydrodynamics and MHD DG2 Riemann problems

HD-DG2	MHD-DG2-Oblique	MHD=DG2-Transversal
DG2 and $\mathbf{B} \equiv 0$	DG2 and $\mathbf{B} = (0.31, 0.31, 0)$	DG2 and $\mathbf{B} = (0, 0.43, 0)$

where negative values of the fundamental derivative appear. The nonlinearity term profile also presents negative values in the same region since the nonlinearity and the fundamental derivative share sign in hydrodynamics (29). From the simulation we have that $\mathcal{G}_{\min} = -0.8554$ and the density and the square of the acoustic sound speed at the same location are $\rho_* = 0.7781$ and $a_*^2 = 0.2981$.

Second and third rows of Figure 1 include MHD simulations with initial values as shown in Table III. The initial values of magnetic field for each simulation have been calculated following practical criteria 1 and 2.

From criterion 1 we obtain $r = a_*^2 \rho_* = 0.4816$ from where we choose an oblique magnetic field of 45° setting $B_x = B_y \approx r \cos(\frac{\pi}{4})$. We set $B_x = B_y = 0.34$ constant in the whole domain. Results of the MHD Riemann problem are displayed in the second row of Figure 1.

Taking into account the same hydrodynamics scenario, practical criterion 2 determines that applying a transversal magnetic field $\mathbf{B} = (0, B_y, 0)$ with $B_y > 0.3637$ the wave structure will become classical. We set $B_x = B_z = 0$ and $B_y = 0.45$ constant. Results are displayed in the third row of Figure 1.

Both MHD simulations show classical wave structure. In both cases the nonlinearity factors are entirely positive in spite of the phase transition reflected in the profile of the fundamental derivative. The composite wave that appears in the hydrodynamics simulation in the first row of Figure 1 is transformed into a simple expansion fan in the MHD simulations in second and third rows of the same Figure. We also observe the more involved wave structure in the MHD-DG1-Oblique simulation in second row due to the presence of the x-component of the magnetic field. Four nonlinear waves appear, two at each side of the entropy wave.

2. DG2 hydrodynamic and MHD Riemann problems

The initial data of the DG2 hydrodynamics Riemann problem are displayed in Table II. The value of the fundamental derivative at the initial time is negative at both sides of the interface. This example represents the case where the flow field remains with negative fundamental derivative during the flow evolution. This issue, in the hydrodynamics case, implies that the nonlinearity is also negative everywhere and therefore the wave dynamics is entirely non-classical.

We compute the solution at time $t_* = 0.45$. Figure 2 includes the hydrodynamic and MHD simulations. First row displays the hydrodynamic results. We observe non-classical phenomena as nonlinear waves appear in reverse form: an expansion shock propagating to the left and a compression fan propagating to the right. From this simulation we compute the required values to apply our practical criteria and determine the amount of magnetic field to revert the non-classical behavior into a classical regime. We obtain $\mathcal{G}_{\min} = -1.3179$ and $\rho_* = 0.7807$ and $a_*^2 = 0.2445$ in the same location.

Following criterion 1 we have that $r = a_*^2 \rho_* = 0.4816$ from which we prescribe an oblique magnetic field of 45° setting $B_x = B_y = r\,\cos(\frac{\pi}{4}) \approx 0.31$.

Criterion 2 for this problem states a transversal magnetic field where $B_y > 0.4095$. We set $B_x = B_z = 0$ and $B_y = 0.43$ constant. Initial data of the MHD-DG2 Riemann problems are summarized in Table IV and results are displayed in second and third row of Figure 2 respectively.

In both MHD simulations we observe a classical wave structure: rarefactions moving to the left, and shocks moving to the right side of the flow field. The nonlinearity terms exhibit positive values in both problems while the fundamental derivative remains negative in the whole domain. We also observe a more involved wave structure in the oblique case as expected because of the presence of the x-component of the magnetic field.

3. DG3 hydrodynamic and MHD Riemann problems

Initial data of problem DG3 are included in Table II. This initial data present a phase change since $\mathcal{G}_L = -0.031$ and $\mathcal{G}_R = 0.703$. The solution of the hydrodynamic problem at time $t_* = 0.2$ exhibits a three wave structure: a contact (entropy) wave separating

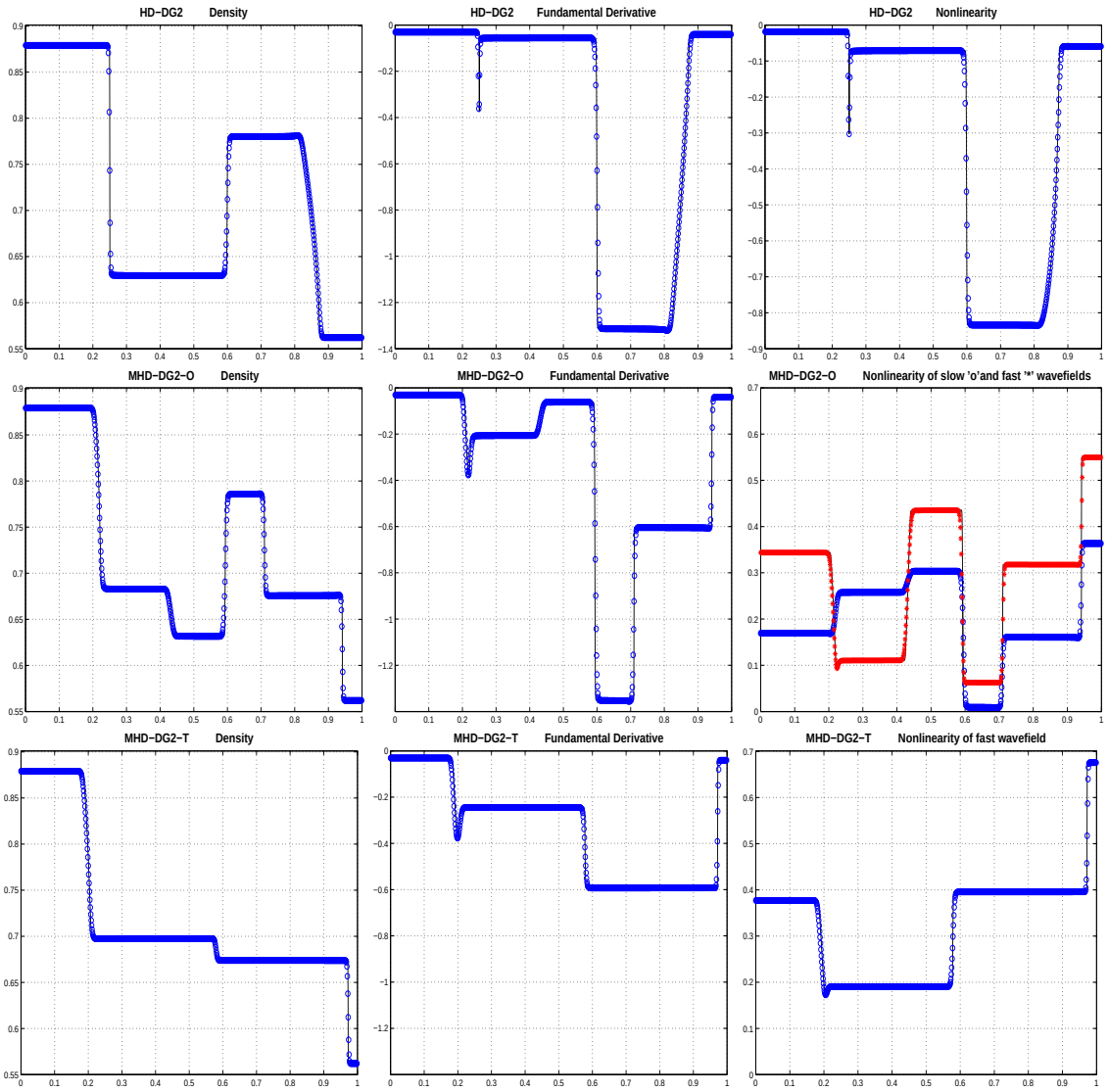

FIG. 2. Numerical solutions at time $t = 0.45$ of the Hydrodynamics and MHD van der Waals DG2 Riemann problems. First row, Hydrodynamics-DG2. Second row, MHD-DG2 with Oblique magnetic field. Third row, MHD-DG2 with Transversal magnetic field. Form left to right profiles of: density, fundamental derivative and the corresponding nonlinearity factors of nonlinear wavefields for each case.

a compression shock wave traveling to the right and a composite wave traveling to the left consisting of an expansion shock attached to an expansion fan. The structure of the composite wave is located in the position where the fundamental derivative changes sign. The nonlinearity factor presents a similar profile as the fundamental derivative and becomes negative at the same locations since both share sign in the hydrodynamic case (29). From the

TABLE V. Initial data for Hydrodynamics and MHD DG3 Riemann problems

HD-DG3	MHD-DG3-Oblique	MHD-DG3-Transversal
DG3 and $\mathbf{B} \equiv 0$	DG3 and $\mathbf{B} = (0.4, 0.6, 0)$	DG3 and $\mathbf{B} = (0, 0.38, 0)$

simulation we obtain $\mathcal{G}_{\min} = -0.3733$ and the values for density and square of the acoustic sound speed at the same location are $\rho_* = 0.7703$ and $a_*^2 = 0.3910$ respectively. With these values we use the practical criteria to determine different amounts of magnetic field to revert non-classical wave phenomena into classical.

The initial data for the MHD-DG3 are shown in Table V. The initial values of the magnetic field have been estimated satisfying practical criteria 1 and 2.

From practical criterion 1 we have that $r = a_*^2 \rho_* = 0.5488$. This value provides an estimation of the radius of the corona region where the total magnitude of magnetic field needs to be defined to counterbalance negative values of the fundamental derivative. In this example we choose a magnetic field in the corona region setting $B_x = 0.4$ and $B_y = 0.6$ which gives $\mathbf{B}^2 = 0.52$. Results are displayed in the second row of Figure 3.

Practical criterion 2 states $B_y > 0.2738$ and we set the magnetic field as $B_x = B_z = 0$ and $B_y = 0.38$ constant. Third row of Figure 3 exhibits the results for this MHD test.

We observe positive nonlinearity factors in both, oblique and transversal, MHD computations. In spite of the phase transition that takes place in the interval $]0.3, 0.4[$, reflected with a change of sign of the fundamental derivative, there is not thermodynamical composite wave showing up in the MHD quantities because both nonlinearity factors are positive. The composite wave appearing in the hydrodynamics case (represented in the first row of Figure 3) is transformed in second and third rows into simple expansion fans.

In the three examples presented up to this point we have added positive amounts of magnetic field in the initial states of the evolution of the hydrodynamic systems. The magnetic field has dissolved thermodynamical composite waves induced by phase transitions transforming anomalous phenomena in the wave structure in the hydrodynamic simulations into classical regimes in the MHD framework. In each example we have reverted a situation where the nonlinearity was negative in some regions of the domain to the case where the nonlinearity terms associated to nonlinear wavefields in MHD were entirely positive.

As mentioned in Section III it is well known in MHD systems that the rotation of the

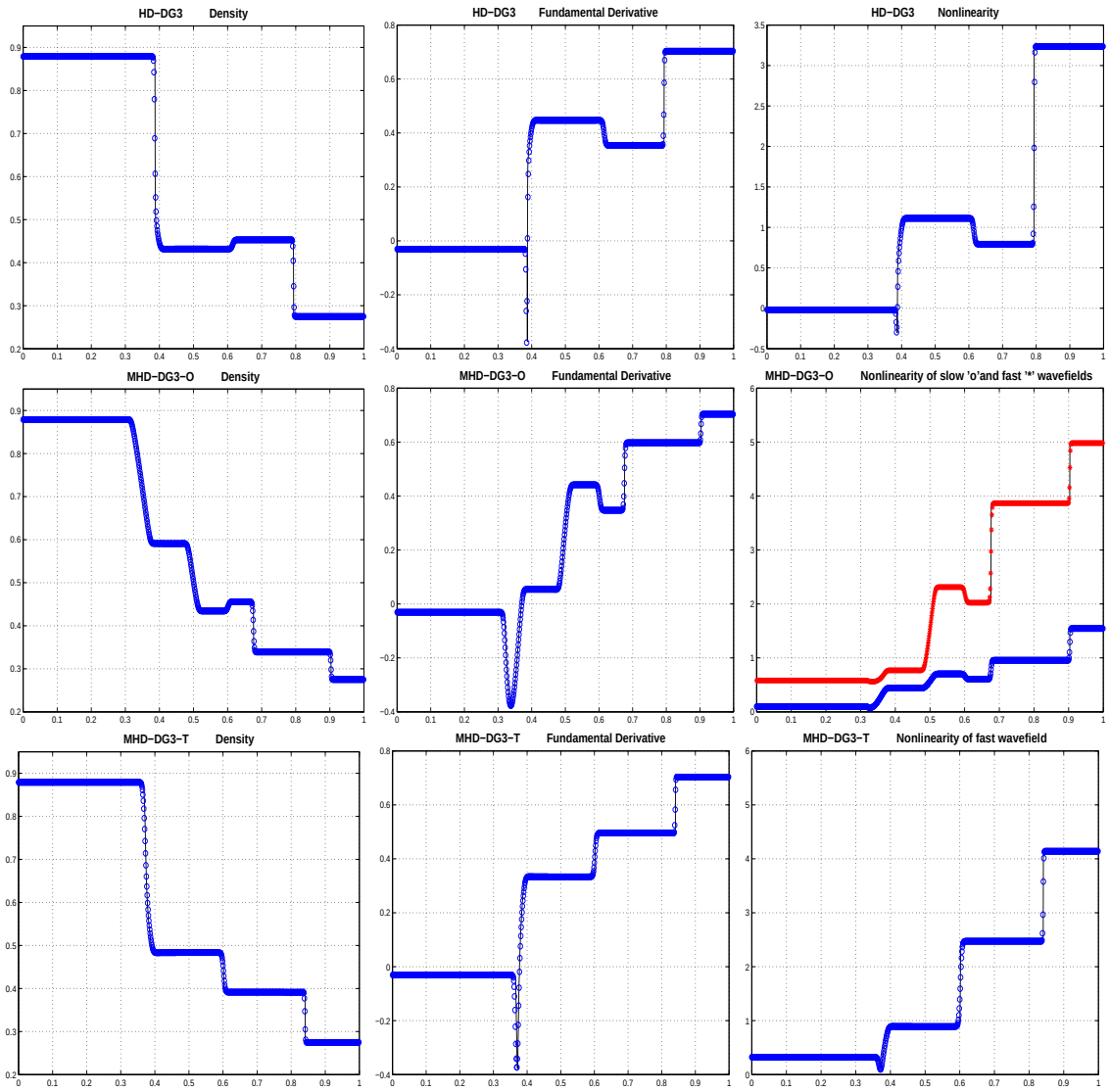

FIG. 3. Numerical solutions at time $t = 0.2$ of the Hydrodynamics and MHD van der Waals DG3 Riemann problems. First row, Hydrodynamics-DG3. Second row, MHD-DG3 with Oblique magnetic field. Third row, MHD-DG3 with Transversal magnetic field. Form left to right profiles of: density, fundamental derivative and the corresponding nonlinearity factors of nonlinear wavefields for each case.

magnetic field might induce non-genuinely nonlinearity in some of the nonlinear wavefields. The loss of genuniely nonlinearity entails the consequent anomalous wave structure in the form of composite waves[5,6,8,40].

In the next example we consider a case where the magnetic field rotates. We add to the DG3 problem initial data a transversal magnetic field with change of sign in the y-direction

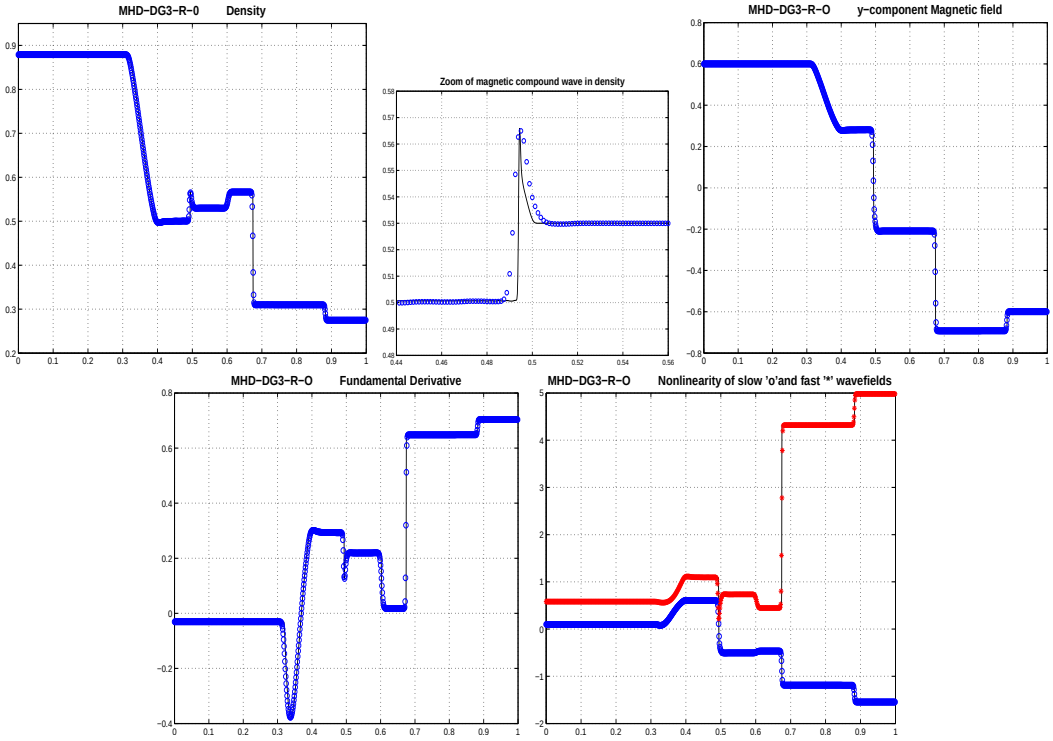

FIG. 4. Numerical solution at time $t = 0.2$ of the MHD van der Waals DG3 Riemann problem with Rotated Oblique magnetic field. Profiles of density, zoomed region for the compound wave in density, y-component of the magnetic field, fundamental derivative and nonlinearity factors of nonlinear wavefields

which will induce a magnetic composite wave. This example shows that the anomalous wave behavior in MHD systems is independent from the EOS model used.

4. Planar MHD-DG3 Riemann problem with rotating magnetic field

We consider the hydrodynamics initial data DG3 together with a magnetic field that has a change of sign in the y-component, $\mathbf{B}_L = (0.4, 0.6, 0)$ and $\mathbf{B}_R = (0.4, -0.6, 0)$. Let us remark that the total amount of magnetic field in this problem is the same as in the previous MDG3-0blique problem. The difference relies on the minus sign of the y-component at the right side of the interface. This change of sign implies rotation of the magnetic field and the subsequent formation of a magnetic composite wave[5,40].

We compute the approximate solution at time $t_* = 0.2$ and display results in Figure 4. Similarly as in the previous example the total amount of magnetic field ($\mathbf{B}^2$) counterbalances

the negative value of the fundamental derivative in the expression of the nonlinearity factor (17) implying the suppression of the thermodynamical composite wave that was originally in the hydrodynamic DG3 example in first row of Figure 3.

In Figure 4 we observe a phase transition in the interval $]0.3, 0.4[$ but not anomalous structure appears in the same region in the density profile. This is because both nonlinearity factors are positive in the interval. However we recognize a magnetic composite wave in the region $]0.48, 0.52[$ where B_y changes sign. A zoomed region of the anomalous structure in density is displayed at the center of the first row of the Figure. The generation of this composite wave is due to the rotation of the magnetic field and not because of thermodynamic effects (fundamental derivative is positive in $]0.48, 0.52[$). Let us remark that this composite wave has the same structure as the one appearing in ideal MHD systems under a rotating magnetic field[5,6,8,40,44].

This is an illustrative example of the way the magnetic field influences the wave structure of the MHD system. While the total amount of $\mathbf{B}$ has balanced out the negative weight of the fundamental derivative in the nonlinearity term dissolving the thermodynamic composite wave, its rotation caused by a change of sign in the y-component has induced negative values in the nonlinearity term (17).

5. Planar MHD-DG3 Riemann problem with large amount of magnetic field: $B_x = 1$ and $B_y = 1$ constant.

In this example we consider the DG3 hydrodynamics initial data together with a large amount of magnetic field in an oblique direction. We evolve the initial data DG3 together with a constant magnetic field $\mathbf{B} = (1, 1, 0)$ in the interval $[-0.5, 1.5]$.

Let us remark that B_y remains positive at both sides of 0.5 and therefore no magnetic composite wave formation is expected. We display in Figure 5 the profiles of the density, fundamental derivative and both nonlinearity factors corresponding to the slow and fast wavefields of the solution at time $t_* = 0.2$ with 1000 points.

We observe a thermodynamical composite wave in the density profile in the same region as the fundamental derivative changes sign. The nonlinearity factor of the slow wavefield reflects the behavior of the fundamental derivative changing sign accordingly. This induces non-classical behavior and the formation of the anomalous structure. The nonlinearity

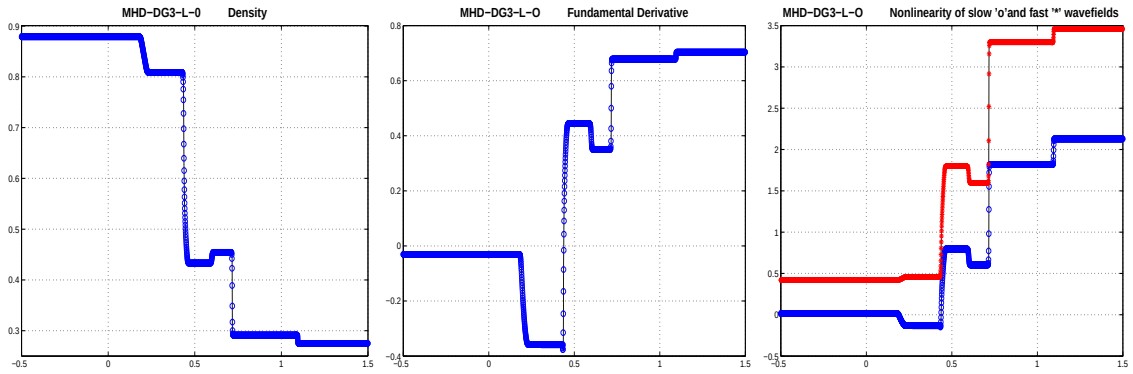

FIG. 5. Numerical solution at time $t = 0.2$ of the MHD van der Waals DG3 Riemann problem with large amount of oblique magnetic field. Profiles of density, fundamental derivative and nonlinearity factors of nonlinear wavefields

term changes sign once, therefore the composite wave consists only of two components: a compression fan attached to a shock wave. In this example the amount of oblique magnetic field is out of the corona region defined in Corollary 1 and is not the appropriate one to cancel out the negative value induced by the fundamental derivative and avoid the formation of the thermodynamic composite wave.

B. A Mie-Grüneisen model for fluids under the influence of magnetic field

The Mie-Grüneisen type EOS is usually considered to model solid and liquid materials in hydrodynamics and is commonly adopted for reactive problems in which detonations arise in solids. The Mie-Grüneisen EOS is specially interesting for the studies of shock waves with multiple phase transitions and mixtures at high pressures and is used to model condensed phase materials to effectively describe the hydrodynamic shock response of many materials included metals[1,15–17,41,42]. In this Section we consider a particular case of this formulation representing a fictitious material called "Bizarrium" proposed in Refs.[41,42] and extensively studied in Ref.[42]. The Bizarrium EOS is built such that the material describes wave propagation with continuous changes of concavity in the isentropes. Phase transitions are reflected through a change of sign in the fundamental derivative and exhibiting a complex wave structure.

We define the pressure following the notation presented in Ref.[42] as

$$P = P_{k0}(\rho) + \Gamma_0\rho_0(\varepsilon - \varepsilon_{k0}(\rho)) \tag{33}$$

with

$$\varepsilon_{k0}(\rho) = \varepsilon_0 - C_{v0}T_0(1 + g(\rho)) + \frac{K_0}{2\rho}x^2 f_0(\rho) \tag{34}$$

$$g(\rho) = \Gamma_0\big(1 - \frac{\rho_0}{\rho}\big) \tag{35}$$

$$f_0(\rho) = \frac{1 + (\frac{s}{3} - 2)x + qx^2 + rx^3}{1 - sx} \tag{36}$$

$$P_{k0}(\rho) = -\varepsilon'_{k0}(\rho) \tag{37}$$

where $x = \frac{\rho}{\rho_0} - 1$ and ρ_0, T_0, Γ_0 and C_{v_0} are the density, temperature, Grüneisen coefficient and the specific heat at constant volume of the reference state respectively.

The thermodynamic quantities relevant in our study are the square of the acoustic sound speed

$$a^2 = \frac{1}{\rho^2}\Big(\Gamma_0\rho_0(P - P_{k0}(\rho)) - P'_{k0}(\rho)\Big) \tag{38}$$

the Grüneisen coefficient

$$\Gamma = \Gamma_0\frac{\rho_0}{\rho} \tag{39}$$

and the fundamental derivative

$$\mathcal{G} = \frac{1}{2}\frac{1}{\gamma\rho^2 P}\Big(P''_{k0}(\tau) + \big(\rho_0\Gamma_0\big)^2(P - P_{k0}(\rho))\Big) \tag{40}$$

where

$$\gamma = \frac{1}{\rho P}\Big(\Gamma_0\rho_0(P - P_{k0}(\rho)) - P'_{k0}(\rho)\Big) \tag{41}$$

Other functions presented in Ref.[42] and needed for the computation of the above quantities are

$$f_1(x) = f'_0(x) = \frac{\frac{s}{3} - 2 + 2qx + 3rx^2 + sf_0(x)}{1 - sx} \tag{42}$$

$$f_2(x) = f''_0(x) = \frac{2q + 6rx + 2sf'_0(x)}{1 - sx} \tag{43}$$

$$f_3(x) = f'''_0(x) = \frac{6r + 3sf''_0(x)}{1 - sx} \tag{44}$$

Similarly, from Eq. (34) we get

$$
\begin{aligned}
P_{k0}(\rho) &= -C_{v0}T_0\Gamma_0\rho_0 + \frac{K_0 x(1+x)^2}{2}\big(2f_0 + xf_1\big)\\
P'_{k0}(\rho) &= -\frac{K_0(1+x)^3\rho_0}{2}\big(2(1+3x)f_0(x) +\\
&\qquad 2x(2+3x)f_1(x) + x^2(1+x)f_2(x)\big)\\
P''_{k0}(\rho) &= -\frac{K_0(1+x)^4\rho_0^2}{2}\big(12(1+2x)f_0(x)\\
&\qquad +6(1+6x+6x^2)f_1(x)\\
&\qquad +6x(1+x)(1+2x)f_2(x) + x^2(1+x)^2 f_3(x)\big)
\end{aligned}
$$

As stated in Ref.[42] the domain of validity of this EOS is determined by relevant values of the reference potential and thermodynamic stability. These conditions provide that the density must be restricted between 8113.102 and 16666.666 kg/m^3.

From expression (40) it can be checked that the change of sign of the fundamental derivative happens twice. Indeed, the loss of convexity of the Bizarrium EOS occurs when the density ρ varies in the interval $[11428, 13333]$

In the following we analyze a test problem proposed in Ref.[42] for Euler equations ruled by the Mie-Grüneisen EOS. We reproduce the hydrodynamic results and extend the data to a MHD test adding specific amounts of magnetic field such that the anomalous wave structure originally present in the hydrodynamic problem is dissolved.

1. Bizarrium test for hydrodynamics

We consider the so-called Bizarrium test problem for hydrodynamics presented in Ref.[42]

$$
(\rho, u, P) = \begin{cases} (14285.7, 0, 10^{11}); & x \leq 0.5 \\ (10000, 250, 0); & x > 0.5 \end{cases}
$$

with parameters as showed in Table VI.

This test problem has been designed to exhibit composite wave structure at both sides of the entropy wave. The initial state consists of two states where the fundamental derivative is positive and the jump discontinuity in 0.5 contains two points where $\mathcal{G}$ changes sign.

The complex wave structure appearing in the evolution of this initial data is considered a benchmark to evaluate the behavior of numerical methods[42]. Before considering an exten-

TABLE VI. Coefficients of the Bizarrium EOS

ρ_0 (kg/m^3)	10000	s	1.5
K_0 (Pa)	10^{11}		
C_{v_0}(J/kg/K)	1000	q	$-\frac{42080895}{14941154}$
T_0 (K)	300		
ε_0(J/kg)	0		
S_0	0	r	$\frac{727668333}{149411540}$
Γ_0	1.5		

sion of this problem to MHD scenarios we approximate the solution of the hydrodynamics problem to test the robustness of the numerical scheme.

We compute the approximate solution at time $t_* = 8 \cdot 10^{-5}$ using 1000 grid points and CFL= 0.8. Figure 6 displays the profiles of the density, velocity, pressure, fundamental derivative and nonlinearity factor. We observe composite waves at both sides of the entropy wave. The rarefaction fan traveling to the left splits into two branches that are connected through an expansion shock. The shock wave traveling to the right splits into two compression shocks connected through a compression fan.

We calculate the value of the fundamental derivative from the computed values of the conserved variables at final time of the evolution. We observe that the profile of the fundamental derivative presents a numerical artifact near the entropy wave. The "spike" reaches negative values which are non-physical. This numerical effect is the result of the evolution of a startup error which occurs when the initial data includes a phase change as is the case in the Bizarrium test. The formation of the nonlinear wave that propagates away from the entropy wave generates the "spike" due to the presence of numerical diffusion. This numerical artifact cannot generate spurious composite waves because entropy waves are linear waves and the theory states that anomalous wave structure is only developed around nonlinear waves. This effect is also reflected in the profile of the nonlinearity factor.

Our interest focuses on transforming the appearing non-classical wave structure into a classical one. In the next example we add a specific amount of magnetic field in the initial states of the evolution to perturb the complex wave structure induced by phase transitions.

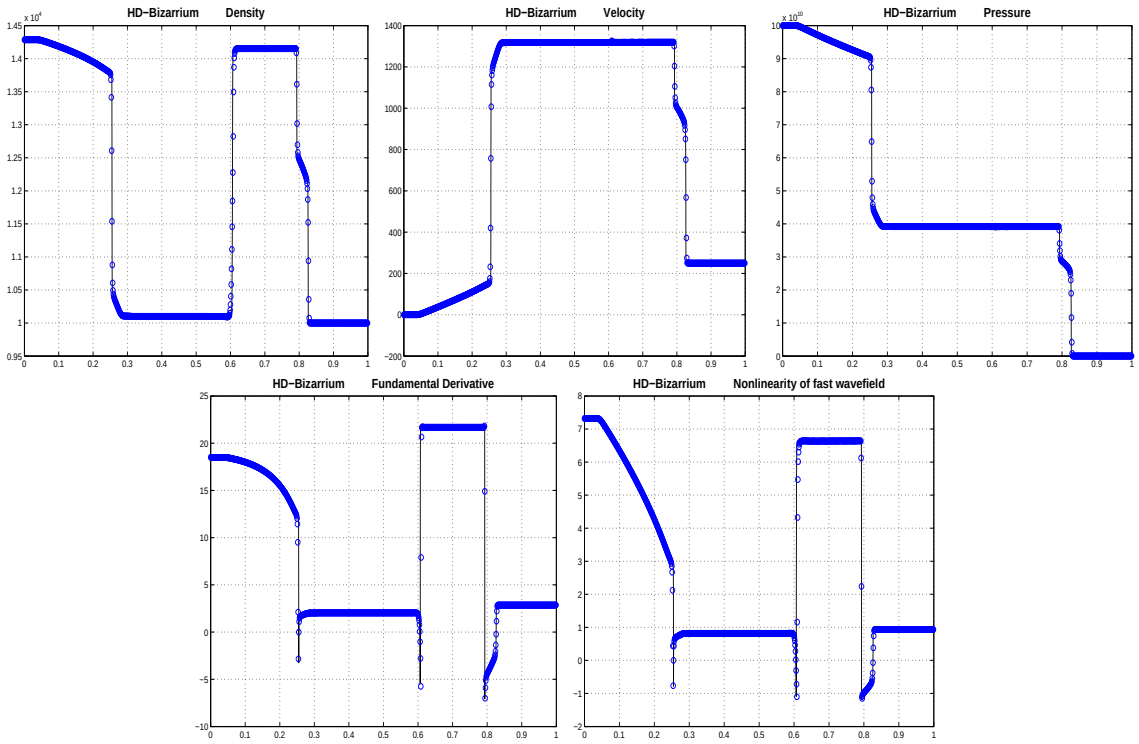

FIG. 6. Numerical solution at time $t = 8 \cdot 10^{-5}$ of the Bizarrium test for hydrodynamics. Top to bottom and left to right profiles of density, velocity, pressure, fundamental derivative and nonlinearity factor of the nonlinear wavefield at time.

2. MHD Bizarrium test

The evolution of the hydrodynamics Bizarrium initial data problem at time $t_* = 8 \cdot 10^{-5}$ presents anomalous structure supported by negative values of the nonlinearity which are induced by the fundamental derivative. The thermodynamical variable provides a profile with minimum value equal to $\mathcal{G}_{\min} = -7.0725$. In order to determine an amount of magnetic field to counterbalance this value and obtain positive nonlinearity terms in the magnetohydrodynamics framework we use the criteria presented at the beginning of this section. Since the minimum value of the fundamental derivative is smaller than $-\frac{3}{2}$ the possibility of reverting the non classical wave structure into a classical one by using a oblique magnetic field is excluded and the only way to revert it is by determining a transversal magnetic field as suggested in practical criterion 2.

The values of the density and square of the acoustic sound speed at the same location where the fundamental derivative reaches its minimum value are $\rho_* = 1.2591 \cdot 10^4$ and

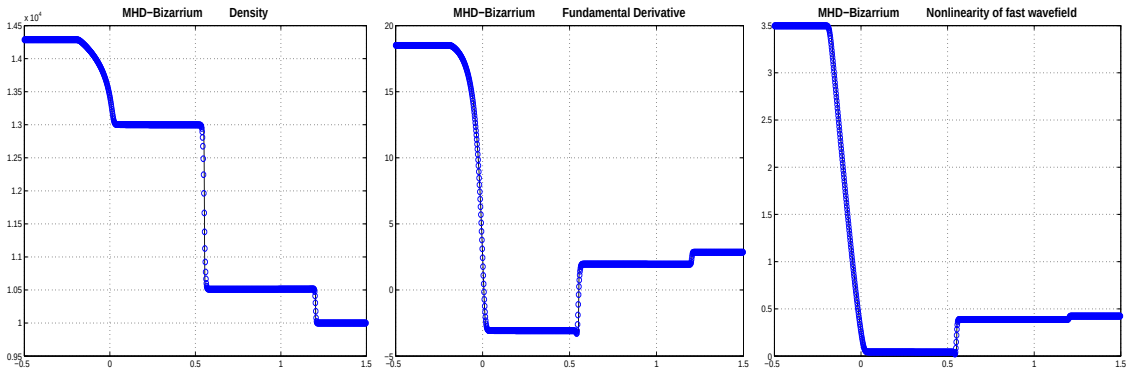

FIG. 7. Numerical solution at time $t = 8{\cdot}10^{-5}$ of the MHD Bizarrium test with constant Transversal magnetic field. Profiles of density, fundamental derivative and nonlinearity factor of the nonlinear wavefield.

$a_*^2 = 4.5716 \cdot 10^6$. From this quantities criterion 2 determines $B_x = 0$ and $B_y > 5.20970 \cdot 10^5$. We initiate the MHD Bizarrium test considering the hydrodynamics initial data together with $B_x = B_z = 0$ and prescribing $B_y = 7.5 \cdot 10^5$ constant in the domain. We compute the approximate solution in the interval $[-0.5, 1]$ at time $t_* = 8 \cdot 10^{-5}$ with 1000 grid points. Figure 7 displays the profiles of the density, fundamental derivative and nonlinearity factor of the fast wavefield (the slow wavefield degenerates to linear). We observe a classical wave structure. One expansion fan travels to the left and one compression shock does to the right of the entropy wave. The slow wave degenerates to the linear entropy wave. The composite wave that appeared in the hydrodynamic case has been dissolved because of the effect of the magnetic field.

We note that the initial constant value of the transversal magnetic field has not only reverted the non-classical waves structure into a classical regime but it has also transformed a blast wave hydrodynamics scenario into a typical shock tube profile.

V. CONCLUSIONS

We have presented an analytical study of the wave structure of MHD system of equations closed with a general EOS. We have proposed a complete spectral decomposition of the fluxes of the system and derived an expression of the nonlinearity factor for the nonlinear wavefields. We demonstrate that the non-ideal MHD wave structure depends crucially on both: the EOS characterizing the material and the magnetic field and its possible rotation.

We prove that phase transitions induced by materials properties might not imply the loss of genuinely nonlinearity. We also show that complex wave structure induced by thermodynamical properties can be neutralized by prescribing a specific amount of magnetic field. We present numerical experiments consisting of a set of one-dimensional Riemann problems for two non-convex EOS that exhibit phase transitions and anomalous behavior in the evolution. In the experiments we show how the non-convex thermodynamic behavior induced by a non-convex EOS in a hydrodynamics system can be reverted into convex dynamics by introducing an appropriate intensity of magnetic field in the system.

VI. ACKNOWLEDGEMENTS

Authors acknowledge financial support by project MICINN-MTM2011-28043. First author also acknowledges support from grants MICINN "Programa Ramón y Cajal", MICINN MTM2011-26995-C02-01 and from the Institute for Pure and Applied Mathematics (UCLA) 2012 program on "Computational Methods in High Energy Density Plasmas".

Appendix A: A numerical scheme for general MHD

A one dimensional numerical scheme in conservation form for a system of conservation laws can be written as

$$\mathbf{u}_j^{n+1} = \mathbf{u}_j^n - \frac{\Delta t}{\Delta x}\big(\tilde{\mathbf{f}}_{j+\frac{1}{2}} - \tilde{\mathbf{f}}_{j-\frac{1}{2}}\big) \tag{A1}$$

where $\mathbf{u}_j^n \approx \mathbf{u}(x_j, t_n)$ is a numerical approximation of the solution in the computational cell $x_j = jh$, $t_n = n\Delta t$ where h and Δt are the spatial and time step sizes respectively and $\tilde{\mathbf{f}}_{j+\frac{1}{2}}$ represents the numerical flux.

The specific form of the first order accurate approximation of the system of equations reads as

$$\mathbf{u}_j^{n+1} = \mathbf{u}_j^n - \frac{\Delta t}{\Delta x}\big(\tilde{\mathbf{f}}(\mathbf{u}_j^n, \mathbf{u}_{j+1}^n) - \tilde{\mathbf{f}}(\mathbf{u}_{j-1}^n, \mathbf{u}_j^n)\big)$$

such that $\tilde{\mathbf{f}}(\mathbf{u}, \mathbf{u}) = \mathbf{f}(\mathbf{u})$.

The first order accurate Marquina's flux splitting formula to compute $\tilde{\mathbf{f}}$ in terms of two linearizations for each flux and interface reads, as proposed in Ref.[9], as

$$\tilde{\mathbf{f}}(\mathbf{u}_j^n, \mathbf{u}_{j+1}^n) = \sum_{p=1}^{7} \Big(\psi_+^p \mathbf{r}_p^f(\mathbf{u}_j^n) + \psi_-^p \mathbf{r}_p^f(\mathbf{u}_{j+1}^n)\Big) \tag{A2}$$

where ψ_+^p and ψ_-^p represent the lateral numerical characteristic fluxes.

In order to compute the lateral numerical characteristic fluxes we proceed similarly as proposed in Ref.[8] for ideal MHD. The proposed entropy-fix upwind scheme for ideal MHD is proved to behave low dissipative. It is designed such that the upwind strategy is used in each interface unless the interface is located in a region containing sonic points or points where the magnetic field rotates inducing non-convexity of the nonlinear wavefields. In those cases a Local Lax-Friedrichs strategy is proposed by prescribing a local viscosity calculated in terms of the characteristic wave speeds and the magnetoacoustic sound speed.

In the present case of general MHD we extend the mentioned methodology in a way that the Local Lax-Friedrichs strategy is also used when non-convex hyperbolicity is induced by phase transitions, i.e., changes of sign of the fundamental derivative.

The procedure reads as follows. We first compute the complete system of eigenvectors at $\mathbf{u}_j^n$ and $\mathbf{u}_{j+1}^n$ and the associated eigenvalues $\lambda_p(\mathbf{u}_j^n)$ and $\lambda_p(\mathbf{u}_{j+1}^n)$ for $p = 1, 2, \cdots, 7$ as proposed in Section 2. The local characteristic fluxes and variables are calculated at both sides of the interface as

$$\phi_j^p = \mathbf{f}(\mathbf{u}_j^n) \cdot \mathbf{l}_p(\mathbf{u}_j^n)$$
$$w_j^p = \mathbf{u}_j^n \cdot \mathbf{l}_p(\mathbf{u}_j^n)$$

for $p = 1, 2, \cdots, 7$.

Then, a first order computation of the numerical characteristic fluxes ψ_+^p and ψ_-^p is determined at both sides of the interface from the following procedure.

We distinguish three types of interfaces namely: *singular, sonic* and *upwind*. Singular interface is the interface that contains a point of non-convex hyperbolicity, i.e., an isolated point where the nonlinearity factor vanish. A sonic interface is an interface where the characteristic wave speeds change sign, i.e., there is at least one $q \in \{1, 2, \cdots, 7\}$ such that $\lambda_q(\mathbf{u}_j^n) \cdot \lambda_q(\mathbf{u}_{j+1}^n) \leq 0$. An upwind interface is an interface that is neither singular nor sonic.

For the singular and sonic interfaces we compute the lateral numerical characteristic fluxes following a Local Lax-Friedrichs approach as,

$$\psi_+^p = \frac{1}{2}(\phi_j^p + \alpha w_j^p); \qquad \psi_-^p = \frac{1}{2}(\phi_{j+1}^p - \alpha w_{j+1}^p); \tag{A3}$$

for $p = 1, 2, \cdots, 7$. The local viscosity α is computed as

$$\alpha_p = \max(|\lambda_p(\mathbf{u}_j^n)|, |\lambda_p(\mathbf{u}_{j+1}^n)|) \tag{A4}$$

for the sonic interface and as

$$\alpha = \max(|\lambda_4(\mathbf{u}_j^n)|, |\lambda_4(\mathbf{u}_{j+1}^n)|) + \max(c_j, c_{j+1})$$

where

$$c_i = \sqrt{c_f(\mathbf{u}_i^n)^2 + c_s(\mathbf{u}_i^n)^2} \quad \text{for} \quad i = j, j+1$$

for the singular case.

Upwind interfaces are solved following the upwind strategy:

- If $\lambda_p(u_j^n) > 0$,

$$\psi_+^p = \phi_j^p; \qquad \psi_-^p = 0 \tag{A5}$$

- If $\lambda_p(u_j^n) \leq 0$,

$$\psi_+^p = 0; \qquad \psi_-^p = \phi_{j+1}^p \tag{A6}$$

for $p = 1, 2, \cdots, 7$.

High order approximation in space can be achieved by computing the numerical characteristic fluxes in terms of $\phi_{j+\frac{1}{2}}^{+p}$, $\phi_{j+\frac{1}{2}}^{-p}$, $w_{j+\frac{1}{2}}^{+p}$ and $w_{j+\frac{1}{2}}^{-p}$ which represent the extended values of the local characteristic fluxes and variables at the interface. This is made by substituting ϕ_j^p by $\phi_{j+\frac{1}{2}}^{+p}$, ϕ_{j+1}^p by $\phi_{j+\frac{1}{2}}^{-p}$, w_j^p by $w_{j+\frac{1}{2}}^{+p}$ and w_{j+1}^p by $w_{j+\frac{1}{2}}^{-p}$.

High order accurate extended values of the local characteristic fluxes and variables are computed following the Shu-Osher flux formulation[47] applying a reconstruction procedure.

In particular, we have implemented the numerical scheme to achieve third order accuracy in space and time. As the reconstruction procedure in space we have used the third order accurate Power Piecewise Hyperbolic Method[48,49] which has a three point stencil. For the integration in time we have utilized the third order accurate TVD Runge-Kutta time stepping procedure proposed in Ref.[47].

The proposed numerical method is stable under a CFL condition[50] determined by

$$\Delta t = C \frac{\Delta x}{\max(|u| + c_f)} \tag{A7}$$

Remark 5 *An alternative method to compute the numerical characteristic fluxes ψ_+^p and ψ_-^p consists on solving all interfaces following the Local Lax-Friedrichs approach. This option is computationally simpler although more dissipative than the proposed one.*

REFERENCES

[1]Menikoff, R, Empirical Equations of State for solids in: ShockWave Science and Technology Reference Library Eds. Horie, Yasuyuki, Springer Berlin Heidelberg, 143-188, 2007.

[2]Davidson, PA, Magnetohydrodynamics in materials processing, Annu. Rev. Fluid Mech. 31: 273-300, 1999.

[3]Nellis, W J Dynamic compression of materials: metallization of fluid hydrogen at high pressures, Rep. Prog. Phys. 69 1479, 2006.

[4]Roe, PL Approximate Riemann solvers, parameter vectors, and difference schemes J. Comput. Phys., 43, 2, 357-372, 1981.

[5]Brio M, Wu CC, An upwind differencing scheme for the equations of ideal magnetohydrodynamics J. Comput. Phys., 75, 2, 400-422, 1988.

[6]Jiang, G.S., Wu,C.C, A high-order WENO finite difference scheme for the equations of ideal magnetohydrodynamics, J. Comput. Phys. 150 (2), 561594, 1999.

[7]Powell, KG, Roe, PL, Myong RS, Gombosi,T, deZeeuw, D, An upwind scheme for magnetohydrodynamics, AIAA 12th Computational Fluid Dynamics Conference, San Diego, CA, AIAA-95-1704-CP, pp 661-674, 1995, doi:10.2514/6.1995-1704.

[8]Serna, S, A characteristic-based nonconvex entropy-fix upwind scheme for the ideal magnetohydrodynamic equations, J.Comput. Phys, 228, 4232-4247, 2009.

[9]Donat R and Marquina,A Capturing Shock Reflections: An improved Flux Formula, J. Comput. Phys. 125, 42-58, 1996.

[10]Marti, JM, Muller, E, Font, JA, Ibanez, JM, Marquina A, Morphology and dynamics of relativistic jets, Astroph. Journal, 479, 1,151, 1997.

[11]Zeldovich, YB, Raizer, YP, Physics of shock waves and high temperature hydrodynamics phenomena, vol II, Academic PREss, New York, 1967.

[12]Thompson, P. A., A Fundamental Derivative of Gas Dynamics, Phys. Fluids,14,1843-1849,1971.

[13]Wendroff, B, The Riemann Problem for Materials with Nonconvex Equations of State I: Isentropic Flow, J. Math Anal and Appl. 38, 454-466,1972.

[14]Wendroff, B, The Riemann Problem for Materials with Nonconvex Equations of State II: General Flow, J. Math Anal and Appl. 38, 640-658, 1972.

[15]Mader, CL, Numerical modeling of detonations. University of California Press, 1979.

[16]J. Johnson,JN, Tang,PK, and Forest, CA, Shock-wave initiation of heterogeneous reactive solids. J. Appl. Phys., 57:4323-4334, 1985.

[17]Zhang, J. Jackson, T.L., Buckmaster, J.D., Freund J.B., Numerical modeling of shock-to-detonation transition in energetic materials, Combustion and Flame, 159,1769-1778, 2012.

[18]LeVeque RJ, Mihalas, D, Dorfi, EA, Müller, E, Computational methods for astrophysical fluid flow, Saas-Fee Advanced Courses, 27, Springer-Verlag, New York, 1998.

[19]Serna, S, Marquina A, Capturing shock waves in inelastic granular gases, J. Comput. Phys., 209, 2, 787-795, 2005.

[20]Serna, S, Marquina A, Capturing blast waves in granular flow, Computers and Fluids,36, 8, 1364-1372, 2007.

[21]Velikovich, AL, Giuliani, JL, Zalesak, ST, Thornhill, JW and Gardiner, TA, Exact self-similar solutions for the magnetized Noh Z pinch problem, Phys. of plasmas, 19, 012707, 2012.

[22]Reisman, DB, Toor, A and Cauble, RC, Magnetically driven isentropic compression experiments on the Z accelerator, J App. Phys, v89, 3, 2001.

[23]Thoma, C, Welch, DR, Clark, RE, Bruner, N, MacFarlane, JJ and Golovkin, IE. Two-fluid electromagnetic simulations of plasma-jet acceleration with detailed equation-of-state, Phys. of plasmas, 18, 103507, 2011.

[24]Foster, JM, Wilde BH, Rosen, PA, Williams, RJR, Blue, BE, Coker, RF, Drake RP, Frank, A, Keiter, PA, Khokhlov, AM, Knauer, JP and Perry, TS, High-energy-density laboratory astrophysics studies of jets and bow shocks, The Astroph. Journal, 634, 77-80, 2005.

[25]Carver, RL, Cunningham, AJ, Frank, A, Hartigan, P, Coker, R, Wilde, BH, Foster, J, Rosen, P, Laboratory astrophysics and non-ideal equations of state: the next challenges for astrophysical MHD simulations, High Energy Density Plasmas, 6, 381-390, 2010.

[26]Sun, Z.H.I., Guo, M., Vleugels, J. ,Van der Biest,O. , Blanpain B., Strong static magnetic field processing of metallic materials: A review C. Op, Solid State and Mat. Sci., 16, 5, 254267, 2012.

[27]Obergaulinger, M.; Cerda-Duran, P.; Muller, E.; Aloy, M. A., Semi-global simulations of the magneto-rotational instability in core collapse supernovae, Astronomy and Astrophysics, 498, pp.241-271, 2009.

[28]Argrow, BM, Computational analysis of dense gas shock tube flow, Shock Waves 6:241-248,

1996.

[29]Cramer, MS, Nonclassical dynamics of classical gases, in Nonlinear Waves in Real Fluids, edited by A Kluwick, Springer-Verlag, New York, 91-145, 1991.

[30]Guardone, A. and Vigevano,L. , Roe Linearization for the van der Waals Gas, J. Comp. Phys. 175, 50-78, 2002.

[31]Müller, S, Voss, A, The Riemann problem for the Euler equations with non-convex and nonsmooth equation of state: construction of wave curves, SIAM J. Sci. Comput., 28, 651-681 ,2006

[32]Thompson, P. A. and Lambrakis, K. C., Negative shock waves, J. Fluid. Mech, 60,187,1973.

[33]Menikoff, R and Plohr, BJ The Riemann problem for fluid flow of real materials Rev. Mod. Phys. , Vol. 61, No. 1, January 1989.

[34]Cramer MS, Sen R, Shock formation in fluids having embedded regions of negative nonlinearity, Phys Fluids 29, 2181, 1986.

[35]Cramer MS, Sen R, Exact solutions for sonic shocks in van der Waals gases, Phys. Fluids 30 (2), 377-385, 1987.

[36]Lax, PD Hyperbolic systems of conservation laws 2, Commun. Pure and Applied Mathematics 10, 4, (1957), 537-566.

[37]Lax, PD Hyperbolic systems of conservation laws and the mathematical theory of shocks waves SIAM, Philadelphia, (1973).

[38]Jeffrey A, Taniuti, T Nonlinear wave propagation Academic Press, New York, 1964.

[39]Landau, L. D. and Lifschitz, E. M., Fluid Mechanics vol 6, Oxford, 1987.

[40]Brio M, Wu CC, Characteristic fields for the equations of magnetohydrodynamics, Nonstrictly Hyperbolic Conservation Laws, Contemporary Mathematics, 60, 19-24, 1985.

[41]Heuze, O, Jaouen S and Jourdren H, Wave propagation in materials with non-convex equations of state, in: M. Elert et at . (Eds.), Shock Compression of Condensed Matter, Proceedings of the Conference of the American Physical Society , vol 955, pp 47-50, 2007.

[42]Heuze, O, Jaouen, S, Jourdren, H, Dissipative issue of high-order shock capturing schemes with non-convex equations of state, J. Comp. Phys 228, 833-860, 2009.

[43]Gelfand, IM Some problems in the theory of quasilinear equations American Mathematical Society Translations, Series 2, Vol29, 295–381, 1963.

[44]Wu, CC, Formation, structure and stability of MHD intermediate shocks, J. Geophys. Res., 95, 8149-8175, 1990.

[45]Fedkiw, R., Merriman, B., Donat, R. and Osher, S., The Penultimate Scheme for Systems of Conservation Laws: Finite Difference ENO with Marquina's Flux Splitting, Innovative Methods for Numerical Solutions of Partial Differential Equations, edited by M. Hafez and J.-J. Chattot, pp. 49-85, World Scientific Publishing, New Jersey, 2002.

[46]Stiriba, Y, Marquina, A, Donat, R, Equilibrium real gas computations using Marquina's scheme, Inter. J. Num. Meth. Fluids, 41, 3, 275-301, 2003.

[47]Shu, CW, Osher, S Efficient implementation of essentially non-oscillatory shock-capturing schemes, 2, J. Comput. Phys., 83, 1, 32-78, 1989.

[48]Marquina,A, Local piecewise hyperbolic reconstructions for nonlinear scalar conservation laws, SIAM J. Sci. Comp. 15, 892-915, 1994.

[49]Serna, S A class of extended limiters applied to Piecewise Hyperbolic methods, SIAM J. Sci. Comput., v28 (1), 123-140, 2006.

[50]Courant R and Friedrichs KO, Supersonic flow and Shock waves, Springer, New York, 1999.